



**POLSKIE TOWARZYSTWO
TECHNOLOGÓW ŻYWNOŚCI
ODDZIAŁ MAŁOPOLSKI**

ŻYWNOŚĆ TECHNOLOGIA JAKOŚĆ

SUPLEMENT

Materiały
VII International Starch Convention
Kraków, 12-14 czerwca 1996

Komitet Naukowy:

A.A.C.M. Beenackers	(Groningen)
Janos Holló	(Budapest)
Jay-lin Jane	(Ames, Iowa)
Wolfgang Kempf	(Detmold)
Josef Kodet	(Červená Řečice)
Chang-yi Lii	(Taipei)
Friedrich Meuser	(Berlin)
Werner Praznik	(Vienna/Tulln)
Harald Röper	(Vilvoorde)
Antoni Rutkowski	(Warsaw)
Piotr Tomasiak	(Cracow)

Komitet Organizacyjny:

Piotr Tomasiak (*head*)
Bohdan Achrem-Achremowicz
Mieczysław Pałasiński
Małgorzata Bączkiewicz
Józef Gładkowski
Marek Sikora
Tadeusz Sikora
Beata Sychowska (*secretary*)

Organizatorzy Konferencji:

Polskie Towarzystwo Technologów Żywności Oddział Małopolski
Akademia Rolnicza w Krakowie
Polski Przemysł Ziemniaczany „POLZIEM” Sp. z o.o. w Poznaniu
Institute of Food Technologists (IFT) – Chicago
Komitet Technologii i Chemii Żywności PAN

Redakcja naukowa materiałów: prof. dr hab. Piotr Tomasiak

Wydanie dofinansowane przez Komitet Badań Naukowych

Qst



**POLSKIE TOWARZYSTWO
TECHNOLOGÓW ŻYWNOŚCI
ODDZIAŁ MAŁOPOLSKI**

ŻYWNOŚĆ TECHNOLOGIA JAKOŚĆ

SUPLEMENT

KOLEGIUM REDAKCYJNE:

Dr hab. Tadeusz Sikora - przewodniczący tel. 012/ 33-08-21 w. 21

Mgr inż. Beata Sychowska - sekretarz tel. 012/ 11-91-44 w. 274

WYDAWCA:

POLSKIE TOWARZYSTWO TECHNOLOGÓW ŻYWNOSCI

Oddział Małopolski

© Copyright by Polskie Towarzystwo Technologów Żywności, Kraków 1996

Printed in Poland

ISSN 1425-6959

ADRES REDAKCJI:

31-425 KRAKÓW, AL. 29 LISTOPADA 46

SKŁAD I DRUK:

Wydawnictwo „Akapit”, Kraków

tel./fax (012)66-67-01

SPIS TREŚCI

Od Redakcji	5
Słowo wstępne	7
<i>Jay-lin Jane</i> Structure of Starch Granules	9
<i>Harald Röper</i> Industrial Products from Starch: Trends and Developments.....	19
<i>J. Holló, A. Neszmélyi</i> Conformation of Starch Polysaccharides in Solution. High-field NMR Investigations and Theoretical Calculations.....	21
<i>Danuta M. Napierala, Mariusz Popenda</i> NMR and Computational Comparative Study of the Amylose – Bengal Rose Complexing in DMSO Solution	28
<i>Krzysztof Polewski</i> Computer Modelling of Amylose Hydration Process in the Presence of Bengal Rose	36
<i>Krzysztof Polewski, Danuta Napierala</i> Absorption and Fluorescence Study of Amylose Complex in Cationic Detergent Using Bengal Rose as a Spectroscopic Probe.....	41
<i>Piotr Tomasik, Włodzimierz Zawadzki</i> Starch Fluorescein Complexes	51
<i>Mark F. Zaranyika, Edward Mukudu, Albert T. Chirenje</i> Activation Energy for the Salt Catalyzed Heterogeneous Dilute Acid Hydrolysis of the Difficultly Accessible Portions of Microcrystalline Cellulose	57
<i>Danuta Sucharzewska, Julia Kominiak, Krystyna Nowakowska</i> Modified Starch-Based Preparations with Antiseptic Action	67

OD REDAKCJI

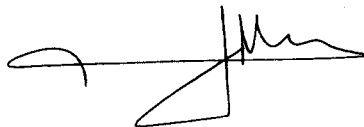
Szanowni Państwo,

Otrzymujecie Państwo *Suplement* do nr 2(7) kwartalnika „*Żywność. Technologia. Jakość.*”, który zawiera materiały prezentowane na VII International Starch Convention (VII Międzynarodowej Konferencji Skrobiowej), a które to referaty z przyczyn niezależnych od organizatorów nie zostały zamieszczone w nr 2(7). Teksty zostały wydrukowane w języku angielskim, ze streszczeniami w języku polskim.

Pragnę poinformować Państwa zainteresowanych tą tematyką, że materiały VII ISC zamieszczone w nr 2(7) i w *Suplemencie* do tego numeru kwartalnika *ŻTJ* zostały przetłumaczone na język polski i aktualnie są przygotowywane do druku.

Kraków, styczeń 1997 r.

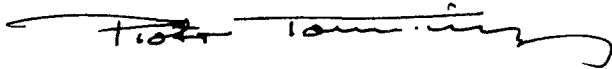
Redaktor Naczelny

A handwritten signature in black ink, consisting of a horizontal line with a loop on the left and a vertical line crossing it, followed by a series of wavy lines on the right.

Tadeusz Sikora

It is my pleasure to offer to the readers a subsequent part of the proceedings of VII International Starch Convention, Cracow 12-14 June 1996. The latest contributions in this issue arrived from the authors in October. I hope that the value of this supplement is due to its scientific content and conservation of the memory of the past meeting. It should also induce the will of participation in the subsequent, VIII ISC, scheduled for 16-19 June 1998 in Cracow. The first circular of this event will be distributed soon.

Prof. Dr. Piotr Tomasik, D.Sc.

A handwritten signature in black ink, appearing to read 'Piotr Tomasik', with a long horizontal flourish extending to the right.

(Editor of this issue)

JAY-LIN JANE

STRUCTURE OF STARCH GRANULES

Abstract

Starch is produced in a semicrystalline granule form by higher plants for energy storage. The granule size and granule shape of starch differ with the botanical source. The diameter of starch granule varies from submicron to more than a hundred microns. The shape of the granules include spherical, oval, disk, polygonal, elongated, and kidney. Starch consists of amylopectin, a highly branched molecule, and amylose, primarily a linear molecule with few branches. Biosynthesis of starch is originated at the hilum, and the starch granule development is by apposition. The amylose content of starch granules increases with the maturity and the size of the starch granule, and amylose is found more concentrated at the periphery of the granule. The branch chain length of amylopectin, however, decreases as the granule size increases. Amylopectin molecules at the hilum consist of exceedingly long branches which are loosely packed with little crystallinity. These long branches are susceptible to iodine to develop a blue core in the granule. The outer chains of amylopectin are in a double helical crystalline structure. Starches which consist of amylopectin with longer branch chains (such as potato and high-amylose maize starches) display the B-type X-ray diffraction pattern, whereas those with shorter branch chains (such as wheat, rice, and maize) display the A-pattern. Starches with branch chain length in between (such as tapioca and banana) display the C-pattern.

Amylose in the granule is dispersed among amylopectin. This is evident as amylose molecules are cross-linked to amylopectin, whereas amylose molecules are not found cross-linked among themselves. The molecular size of amylose increases with the increase of the granular size. Most amylose in the starch granule is present in a free form not complexed with lipids; however, about 21% amylose in non-waxy barley starch is present as lysophospholipid complex.

³¹P-NMR studies have shown that phospholipids are present in all the normal cereal starches investigated but not in tuber, root, and legume starches. With few exceptions (e.g., waxy maize starch), most waxy starches do not contain phospholipids. Phosphate derivatives are primarily on amylopectin. Studies conducted by using DSC, X-ray, chemical analysis, and ³¹P-NMR of Naegeli dextrans showed that a substantial proportion of phosphate derivatives were located within the crystalline region of amylopectin and were protected from exhaustive acid hydrolysis.

Starch is produced by green plants for energy storage and is synthesized in a granular form. Biosynthesis of starch granules takes place primarily in the amyloplast. The biosynthesis of the granule is initiated at the hilum, and the starch granule grows by apposition [1]. Starch granules are densely packed with semi-crystalline structures and have a density of about 1.5 g/cm^3 [2]. Because of this stable semi-crystalline structure, starch granules are not soluble in water. Without gelatinization, starch can absorb water and swell up to 30% of its dry weight. The swelling process is reversible upon drying. The starch granules are effectively stored in seeds, roots, tubers, stems, and leaves. Grain seeds, such as maize kernels, contain up to 75% starch. The stored starch granules can be hydrolyzed by hydrolytic enzymes to glucose, and the glucose is utilized to generate energy during germination and whenever energy is needed. In the granular form, starch can be easily isolated by gravity sedimentation, centrifugation, and filtration, and can be subjected to various chemical, physical, and enzymatic modifications with subsequent washing and processing. Consequently, starch is produced as one of the most economical commodity products.

Starch is a biopolymer and consists of two major components: amylopectin and amylose. Amylopectin is a highly branched molecule, with α 1-4 linked D-glucose backbones and α 1-6 linked branches. Amylose is primarily a linear molecule with α 1-4 linked glucose units. Some amylose molecules, particularly those with large molecular weight, may have up to 10 or more branches [3]. Amylose and amylopectin have different properties. For example, amylose has a high tendency to retrograde and produce tough gels and strong films, whereas, amylopectin, in an aqueous dispersion, is more stable and produces soft gels and weak films. Entanglements between amylose and amylopectin, particularly with the presence of lipids or phospholipids, have been demonstrated to significantly affect the pasting temperature, paste viscosity, stability, and clarity, as well as the retrogradation process.

Other minor components found in starch granules include the intermediate components which have structures in between amylose and amylopectin, starch lipids (including phospholipids), and phosphate monoester derivatives. Phytoglycogen is found in certain varieties of starch, such as the sugary mutant of maize starch. Some of the minor components, such as phosphate monoester derivatives and phospholipids [4], [5], although at low concentrations, can drastically affect the properties of starch pastes and gels. Phosphate monoester derivatives, carrying negative charges at the neutral pH, are found in many starches. Potato starch, consisting of about 0.09% phosphate derivatives, displays extremely high paste viscosity and clarity and a low gelatinization temperature. The unique properties of potato starch are attributed to the charge repelling between the covalently attached phosphate monoester groups.

An understanding of the internal organization of starch granules is crucial for scientists and engineers to optimize reaction conditions for starch chemical, physical, and enzymatic modifications. The knowledge of the internal organization can help us understand the functionalities and the transformation behaviors of starch and improve the properties and stability of starch products. This knowledge will also help biochemists reveal the mechanism by which starch granules are developed during biosynthesis. In this paper, some recent advances in the understanding of the structure of starch granules are reviewed.

Morphology of starch granules

Starches isolated from different botanical sources display characteristic granular morphology [6]. Starch granules have various shapes, including spherical, oval, polygonal, disk, elongated, and kidney shapes. Normal and waxy maize starches are spherical and polygonal in shape. Immature sweet corn starch has a multi-modal size distribution, but starch granules are not found in the mature sweet corn. High-amylose maize starches have elongated and curved rod-shaped granules in addition to polygonal and spherical granules; some granules also have granular appendages. It is not known whether the elongated shape is correlated with the amylose content. Potato starch has oval and spherical shapes. Wheat, triticali, barley, and rye starches have bimodal size distributions. The large (A) granules have a disk shape, whereas the small (B) granules have a spherical shape. Sorghum starch also has a bimodal size distribution, but the shapes are different: large granules of sorghum starch have polygonal and spherical, instead of disk, shapes. Diffenbachia starch has an elongated submarine shape. Shoti starch has a disk shape with sharp edges. Almost all the legume starches have a characteristic indentation on granules of bean-like shapes.

Diameters of starch granules vary from submicron, such as amaranth and small pigweed, to more than one-hundred microns, such as canna starch [6]. Other starches, such as small wheat granules have diameters of 2-3 microns; large wheat granules, 22-36 microns; potato, 15-75 microns; maize, 5-20 microns; rice, 3-8 microns; and legume starches, 10-45 microns [6].

Most starch granules are produced individually in separate amyloplasts; however, some starches, such as rice and oats, have several starch granules produced simultaneously in a single amyloplast. These starches are known as compound starch. The compound starch has granules tightly packed together, which are relatively difficult to separate. The shapes of the compound starch granules are mostly polyhedral, possibly as a result of space constraints during the development of starch granules.

Small-particle starch can be prepared by treating common granular starch with acid to hydrolyze and remove the glucan at the amorphous region [7]. After the acid treat-

ment, the crystallites of the starch granule are detached. With mild attrition, the starch granules break into small particles. The size of the small-particle starch can be in submicrons and is dependent on the conditions of the acid hydrolysis; the more extensive acid hydrolysis, the smaller particle sizes are produced. The small-particle starch displays irregular shapes with strong birefringence when viewed under a polarized light-microscope. The small-particle starch produced from normal maize starch also displays an enhanced A-type X-ray crystallinity.

Structures and locations of amylose in the starch granule

Amylose is easily leached out from swollen granules at a temperature slightly above the gelatinization. Amylose also does not contribute to the total crystallinity of starch granules. All the results indicate that amylose is present in the amorphous region of the granule. Recent studies conducted by Morrison and co-workers [8] by using solid ^{13}C -NMR have shown that up to 21% of amylose in the granule is complexed with lipids at a single helical conformation, and the remaining amylose is in a random coil conformation free of lipids.

Two hypotheses were proposed regarding where and how amylose was located in the granule relative to amylopectin. One was that amylose must be present in a separate compartment from amylopectin; thus, amylose was not susceptible to branching enzyme reactions. The other was that amylose was dispersed among amylopectin; thus, the two molecules are intertwined to hold the integrity of the granule. To test if amylose molecules are present in close proximity in the granule, cross-linking reactions of starch granules were conducted by using various cross-linking reagents of different molecular chain length [9], [10].

Epichlorohydrin (ECH), adipic/acetic anhydrides, and phosphoxy chloride were used at low concentrations (e.g., 0.013% to 0.13%, ECH/starch=w/w), to cross-link native granular starch [9]. The cross-linked starch was then subjected to gel permeation column chromatography to analyze if amylose molecules were cross-linked among themselves which would increase the molecular weight. Results, however, showed that amylose was cross-linked onto amylopectin and co-eluted with amylopectin at the void volume, as indicated by the increase in blue-value of the amylopectin peak. The molecular size of the amylose peak did not increase after cross-linking, indicating that amylose molecules were not cross-linked among themselves. Analyses of the phosphoxy chloride cross-linked starch, by using ^{31}P -NMR, showed that the amylose isolated from the cross-linked starch had only phosphate monoester derivatives but no phosphate diesters (cross-link) [10]. The monoester derivatives of the amylose are responsible for the resistance of the amylose isolated from cross-linked starch to enzyme hydrolysis (Table 1). All these

results suggest that amylose is located adjacent to or intertwined with amylopectin but not in close proximity with other amylose molecules.

Studies of amylose biosynthesis have demonstrated that amylose is synthesized by granular-bound starch synthase, whereas amylopectin is synthesized by soluble starch synthase [11]. Because amylose is synthesized by the granular-bound enzyme, the amylose molecule is likely confined in the granule and has little opportunity to form double helices with other starch molecules to form branches. This biosynthetic pathway also excludes the hypothesis that amylose molecules are separated from amylopectin.

Table 1

Percentage of β -amylolysis of amyloses isolated from native and cross-linked granular corn starch with and without prior isoamylase treatment^{abc}

Treatment	Native Starch	Cross-linked ^d Starch
β -amylase (30 units)	64.6%	53.7%
β -amylase (90 units)	62.8%	54.8%
Isoamylase (328 units) β -amylase (30 units)	85.1%	56.7%

^a Calculated on the basis of total carbohydrate present in maltose peak separated by the Sephadex G-25 column.

^b Amylose was isolated with the Sepharose CL-2B column.

^c Amylose (15 mg) in 15 ml acetate buffer solution (pH5, 20mM), conditions are given in Material and Methods.

^d Cross-linked with 0.25% ECH (ECH/starch = w/w).

Amylose contents of starch granules increase with the maturity and the increase of the granule size (Table 2). Studies conducted by using surface gelatinization of starch granules have shown that amylose molecules isolated from the core of the granule have substantially larger molecular sizes than those at the periphery [12]. These results are consistent with results of starch granules of different granular sizes and maturities. The structural feature of having a large concentration of small-molecular-weight amylose present at the periphery coincides with the phenomenon that small-molecular amylose leach out from the granule soon after starch gelatinization.

Structures and locations of amylopectin in the granule

Amylopectin is a highly branched molecule. There are three types of branch chains. A-chains are linked with other chains (B- or C-) by the reducing ends through α 1-6 bonds, but A-chains do not carry other chains. B-chains are similarly linked to another B-

chain or C-chain, but B-chains also carry A-chains or other B-chains at the C-6 of the glucose unit. Each amylopectin molecule has only one C-chain which carries the sole reducing end of the molecule.

Table 2

Amylose contents of potato starch with different granular sizes and of starch at different radial locations

Sample	Amylose content ^{a,b} (%)
Native potato starch	20.2 ± 0.1
Potato starch (<20 μm ^c)	16.9 ± 0.2
Potato starch (<30 μm ^c)	17.5 ± 0.1
Potato starch (30-52 μm ^c)	20.3 ± 0.1
Potato starch (>52 μm ^c)	20.6 ± 0.1
Remaining granular starch after (80% chemical gelatinization)	18.8 ± 0.1
Remaining granular starch after (52% chemical gelatinization)	19.6 ± 0.1
Chemically gelatinized starch (52% chemical gelatinization)	21.1 ± 0.4
Chemically gelatinized starch (10% chemical gelatinization)	22.0 ± 0.1

^a The amylose content was calculated by dividing the iodine affinity of the sample by 19.9%.

^b Data reported are the means of three replicates.

^c Diameter

Branch chain length of amylopectin varies with the origin and maturity of the starch and the location of molecules in the granule. Hizukuri and co-workers [13] surveyed a wide variety of starch and reported average chain lengths of the starches. It is known that amylopectin makes up the crystalline structure of starch, whereas amylose is in the amorphous form. Starches isolated from potato and high-amylose maize, which comprise long branches, display the B-type x-ray pattern. Other starches isolated from normal and waxy maize and wheat, which comprise short branches, display the A-type pattern. Starches isolated from banana and tapioca, which have average branch chain length in between the A and B starches, display the C-pattern.

Nikuni [14] and French [15] independently proposed the cluster model of amylopectin, in which the branch points are located in clusters and the branch chains are present in double helical crystalline structure. The structure of the amylopectin molecule consists of alternating crystalline and amorphous regions. Kassenbeck [16] studied enzymatically treated starch granules and reported a repeating distance of 70 Å. Yamaguchi

et al. [17] examined wet meshed and acid hydrolyzed waxy maize starch by using transmission electron microscopy and reported a repeating distance of 70 ± 10 Å and lamellae thickness of about 50 Å. The authors proposed that alternating crystalline and amorphous regions of 50 Å and 20 Å, respectively, are arranged in the amylopectin structure of waxy maize starch.

Blanshard et al. [18] observed a Bragg peak at approximately 100 Å by using small-angle neutron scattering studies of starch granules. The Bragg peak disappeared on gelatinization. Recent studies of amylopectin structural periodicity by using small angle X-ray scattering have shown a constant repeating distance of between 8.7 and 9.2 nm for the six starch varieties examined [19]. Results obtained from these two scattering studies show larger repeating distances than those reported by Kassenbeck and by Yamaguchi et al. Blanshard et al. [18] attributed the difference to the drying process of starch samples required for the electron microscopy. There may be shrinkage of starch structures during the drying.

This consistent distance of about 9 or 10 nm coincides with the distances of amylose double helical crystallites and the lamellar distance of amylose single helical complex formed during the biosynthesis, about 10 nm [20]. Whether the repeating distance of amylopectin is controlled by the size of double helix is of great interest to study. Further studies may reveal the mechanism of starch biosynthesis and granule development.

To investigate the structures of amylopectin molecules at different radial locations (e.g., the core and the periphery) of the granule, amylopectin in various starch fractions, separated by surface gelatinization using neutral salt solutions, was isolated and analyzed [12]. Results showed that amylopectin isolated from the core, close to the hilum, has substantially longer long-B branches compared with the amylopectin molecules isolated from other parts of the granule. The amylopectin isolated from the periphery of the granule has the shortest long-B chains (Table 3). These results indicate that the branching frequency increases at the periphery. When stained with iodine, the very long amylopectin branch chains at the hilum results in the dark blue core of waxy barley and waxy potato starch granules.

Starches of the B-type X-ray pattern, such as potato and high-amylose maize, are more resistant to enzyme hydrolysis [21]. Whereas those starches of the A-type are more susceptible to enzyme hydrolysis [21]. The B-type X-ray diffraction corresponds to an orthogonal unit cell packing of starch double helices, which consists of an open channel at the center. The A-type starch has a hexagonal unit cell packing [2]. It is puzzling of how such small differences in the average chain lengths of amylopectins can affect the packing of A- and B-types of starch and resulting in substantially different enzyme digestibility. For example, normal maize amylopectin (DP 19.5) and sweet potato amylopectin (DP 20.4) display the A-type pattern, whereas potato amylopectin (DP 22.4) and

Table 3

Amylopectin branch chain length debranched with isoamylase^a

Amylopectin	Branch chain length, DP ^b	
	Long chain	Short chain
Native potato starch	41.2 ± 1.3	13.2 ± 0.3
Potato starch (< 20 μm ^c)	44.7 ± 1.3	14.7 ± 0.7
Potato starch (30-52 μm ^c)	41.2 ± 1.8	13.2 ± 0.4
Potato starch (> 52 μm ^c)	34.0 ± 1.2	13.4 ± 0.2
Remaining granular starch after 80% chemical gelatin	42.5 ± 1.8	13.1 ± 0.1
Chemically gelatinized starch (20% chemical gelatin.)	32.0 ± 0.8	13.1 ± 0.7

^a Data reported are the averages of duplicate sample and chemical analyses except long chain of large granule (>52 μm) with one sample replication and duplicate chemical analysis.

^b Determined with the three peak fractions, DP = degree of polymerization.

^c Diameter

Tulip (DP 20.9) display B-type pattern [13].

Recent studies conducted in our lab by using Naegeli dextrans of normal maize and potato starches [22] showed that after hydrolysis with 16% sulfuric acid for one, two and three months at 22°C, normal maize Naegeli dextrans consisted of substantially more branches than their potato counterparts. In the early stage of the acid hydrolysis, normal maize starch had a higher degradation rate than potato counter parts. X-ray differential patterns of potato Naegeli dextrans showed increases in reflection peak intensity as the hydrolysis progressed, whereas those of normal maize showed decreases in amorphous background but no significant increase in peak intensity. The results suggested that potato amylopectin had more branches located in the amorphous regions which were more susceptible to acid hydrolysis. Normal maize amylopectin, however, had branch points scattered in both the amorphous and the crystalline regions. After extensive acid hydrolysis, normal maize Naegeli dextrans consisted substantial branches compared with potato counterparts. With the highly clustered branch points, potato amylopectin branch chains could form double helices of less interruption, which are more resistant to enzyme hydrolysis. In addition, the double helices could be arranged into a more perfect crystalline structures after acid hydrolysis which removed the molecular constraint caused by branch structures. With the presence of scattered branch points within the crystallin regions, normal maize amylopectin had less perfect double helical structures. The double

helices of the normal maize starch, containing branches, were more susceptible to enzyme attack.

Phosphorus structures and locations in the granule

Phosphorus in starch is mainly present in two forms: phosphate-monoesters and phospholipids [4, 5]. The two constituents have opposite effects on starch paste properties. Phosphate monoesters, present in potato and other starches, increase the paste clarity and paste viscosity, whereas, phospholipids, found in cereal normal starches, such as wheat, rice, and maize, decrease the paste clarity and viscosity. ^{31}P -NMR spectroscopy has been developed as a useful method to determine the structures and contents of phosphorus in starch [23, 24].

Starch phosphate monoesters in native starches, such as potato and rice, are primarily found in amylopectin [4, 5]; only a trace is found in amylose. About 61% phosphate monoester in potato starch is on the C-6, 38% on the C-3, and possibly 1% on C-2 of the glucose unit. Whereas 80-90% phosphate-monoester in waxy rice starch is on C-6 of the glucose unit [5]. Takeda and Hizukuri [25] reported that potato amylopectin contains one phosphate monoester per 317 glucose units, equivalent to one phosphate in 13 branch chains. The phosphate groups are present in long branch chains (long B-chains, DP about 42) and located more than nine glucosyl residues away from branch points.

Recent studies of our research group showed that Naegeli dextrans of potato starch consisted of a substantial amount of phosphorus (65% remained after 3 months hydrolysis). ^{31}P -NMR spectra showed the structure of the phosphorus in the potato Naegeli dextrans remained the same as that of native potato starch with an additional residual peak of glucose-6-phosphate, a product of acid hydrolysis. This result showed that phosphate-monoester derivatives were present in the crystalline region of potato starch and were protected from acid hydrolysis. The phosphorus content of potato starch was also found inversely proportional to the crystallinity of the starch, which was consistent with that potato starch gelatinization enthalpy-changes decrease with the increase of phosphate content [26].


REFERENCES

- [1] Badenhuisen N.P., Dutton R.W.: *Protoplasma*, **XLVII**, 1956, 156-163.
- [2] Sarko A., Wu H.C.H.: *Starch/Staerke*, **30**, 1978, 73.
- [3] Hizukuri S., Takeda Y., Yasuda M., Suzuki A.: *Carbohydr. Res.*, **94**, 1981, 205.
- [4] Schoch T.J.: *J. Amer. Chem. Soc.*, **64**, 1942, 2954.
- [5] Hizukuri S., Tabata S., Nikuni Z.: *Staerke*, **22**, 1970, 338.
- [6] Jane J., Kasemsuwan T., Leas S., Zobel H.F., Robyt J.F.: *Starch/Staerke*, **46**, 1994, 121.
- [7] Jane J., Shen L., Wang L., Maningat C.C.: *Cereal Chem.*, **69**, 1992, 280.
- [8] Morrison W.R., Tester R.F., Snape C.E., Law R., Gidley M.J.: *Cereal Chem.*, **70**, 1993, 385.

- [9] Jane J., Xu A., Rodosovljivic M., Seib P.A.: *Cereal Chem.*, **69**, 1992, 405.
- [10] Kasemsuwan T., Jane J.: *Cereal Chem.*, **71**, 1994, 282.
- [11] Shannon J.C., Garwood D.L., in: *Starch: Chemistry and Technology*. 2nd Ed. Eds. Whistler, R. L., BeMiller J.N., Paschall E.F., Academic Press. Orlando, FL, 1984, p. 25.
- [12] Jane J., Shen J.J.: *Carbohydr. Res.*, **247**, 1993, 279.
- [13] Hizukuri S., Kaneko T., Takeda, Y.: *Bioch. Biophysica Acta*, **760**, 1983, 188.
- [14] Nikuni Z.: *Starch/Staerke*, **30**, 1978, 105-111.
- [15] French D.J.: *Jpn. Soc. Starch Sci.*, **19**, 1972, 8-25.
- [16] Kassenbeck V.P.: *Starch/Staerke*, **30**, 1978, 40.
- [17] Yamaguchi M., Kainuma K., French D.: *J. Ultrastruc. Res.*, **69**, 1979, 249.
- [18] Blanshard J.M.V., in: *Chemistry and Physics of Baking*, Blanshard, J. M. V. ed.; Royal Soc. of Chem., London, 1986, p. 1.
- [19] Jenkins P.J., Cameron R.E., Donald A.M.: *Starch/Staerke*, **45**, 1993, 417.
- [20] Jane J., Robyt J.F.: *Carbohydr. Res.*, **132**, 1984, 105.
- [21] Fuwa H., Takaya T., Sugimoto Y., in: *Mechanisms of saccharide polymerization and depolymerization*. Ed. Marshall, J.J., Academic Press, New York, NY, 1980, p. 73.
- [22] Kainuma K., French D.: *Biopolymers*, **11**, 1972, 2241.
- [23] Lim S.-T., Kasemsuwan T., Jane J.: *Cereal Chem.*, **71**, 1994, 488.
- [24] Kasemsuwan T., Jane J.: *Cereal Chem.* In revision.
- [25] Takeda Y., Hizukuri S.: *Carbohydr. Res.*, **102**, 1982, 321.
- [26] Muhrbeck P., Eliasson A.-C.: *J. Sci. Food Agric.*, **55**, 1991, 13.

STRUKTURA GAŁECZEK SKROBIOWYCH

Streszczenie

Omówiono strukturę polisacharydów skrobiowych, morfologię gałeczek skrobiowych, rozmieszczenie amylozy i amylopektyny w gałeczkach oraz postać i umiejscowienie w nich fosforu 

HARALD RÖPER

INDUSTRIAL PRODUCTS FROM STARCH: TRENDS AND DEVELOPMENTS*

In 1994 the total EU starch market amounted to 6.1 million tonnes from which 55% has been utilised in the food sector and 45 % in the non-food sector. Starch is used as native starch, as modified starch (thickener, binder, texturizer), as starch hydrolysate, isoglucose (bulk sweetener) or as crystalline dextrose as well as their derivatives like polyols (low caloric/low cariogenic bulk sweetener) for the production of processed food, confectionery, fruit products and beverages. Traditional non-food applications of starches and modified starches are in paper and corrugated board, fermentation & chemical industry and as binders and adhesives. Consumption figures by starch product type as well as by application area (food/non-food) are presented. The industrial raw material starch is available in sufficient amounts and in high purity. Factors influencing physico-chemical properties of native starch are explained. Starch modifications with changes of physico-chemical properties of starch lead to different application properties. In the various application areas, innovative products based on starch have entered/are entering the market thus increasing starch demand. These are health food ingredients, biodegradable, bio-compatible and "CO₂ neutral" detergent components like "APG" surfactants, cobuilder and bleach activators, biodegradable thermoplastic materials for packaging, and tailor-made high performing fermentation feedstocks. Raw material requirements by the industry and options for further research and development are discussed.

R&D options

The following R&D options for the starch industry have been identified:

Using classical plant breeding or modern genetic engineering techniques, the following raw material improvements have been targeted: higher yields per hectare,

Cerestar R&D, Centre of Expertise Basic Research, Eridania Beghin-Say Vilvoorde Research & Development Centre, Havenstraat 84, 1800 Vilvoorde, Belgium

* *The complete paper appeared in Carbohydrates in Europe, 15, 1996, 22-29.*

resistance to plant vermin and diseases, better separability of starch from other grain components and new functional properties of starches. During harvest and during treatment: less damage by heat during grain drying, by moulds and by transport. Improvements in separation and purification by using new technologies, e.g. membrane filtration and chromatography

Product innovation

These are new products based on starch using "new enzymes", higher performing products and synergistic product combinations, especially for the food sector (convenience food, light/health food ingredients), detergent components, raw materials for cosmetics, raw materials for the pharmaceutical industry, raw materials for the fermentation industry and biodegradable packaging materials.

PRZEMYSŁOWE PRODUKTY ZE SKROBI - KIERUNKI ROZWOJU

Streszczenie

W 1994 roku na całym rynku Unii Europejskiej znajdowało się do 6,1 miliona ton skrobi z których 55% wykorzystano w sektorze spożywczym a 45% w sektorze niespożywczym. Skrobia jest stosowana jako skrobia natywna, modyfikowana (zagęstnik, środek wiążący lub teksturyzujący), jako hydrolizat skrobiowy, izoglukozę (słodzik) lub jako krystaliczna dekstroza i ich pochodne jak poliole (niskokaloryczny środek słodzący) do produkcji obrobionej żywności, bakalii, produktów owocowych i napojów alkoholowych. Tradycyjnymi zastosowaniami niespożywczymi skrobi i modyfikowanych skrobi są papier, tektura falista, fermentacja i przemysł chemiczny, środki wiążące i adhezyjne. Przedstawiono wielkość zużycia poszczególnych produktów oraz obszary zastosowań spożywczych i niespożywczych. Skrobia jest dostępna w wystarczającej ilości jako wysokiej czystości surowiec przemysłowy.

Wyjaśniono rolę czynników wpływających na fizykochemiczne właściwości natywnej skrobi. Modyfikacje skrobi zmieniające jej fizykochemiczne właściwości prowadzą do różnych zastosowań. W dziedzinie różnych zastosowań weszły na rynek nowe produkty co zwiększyło zapotrzebowanie na skrobię. Są to dodatki do zdrowej żywności, biodegradowalne, biokompatybilne nie zwiększające poziomu CO₂ składniki detergentów jak APG, aktywatory wiązania i bielienia, biodegradowalne termoplastyczne materiały opakowaniowe oraz wysokowydajne pożywki fermentacyjne. Omówiono wymagania stawiane surowcom przemysłowym oraz opcje dla dalszych badań i wdrożeń. ☒

J. HOLLÓ, A. NESZMÉLYI

CONFORMATION OF STARCH POLYSACCHARIDES IN SOLUTION. HIGH-FIELD NMR INVESTIGATIONS AND THEORETICAL CALCULATIONS

Abstract

Interest in the structure and conformation of starch polysaccharides - having either academic or industrial motivation - is not diminishing. Aqueous solutions challenge new experimental techniques.

Results of high-field NMR measurements are reported related to maltooligomers. Unambiguous spectral assignments were obtained and it was found that all monomeric subunits have the 4C_1 conformation. ^{13}C relaxation times (T_1) show remarkable flexibility (0.3 sec at 80°C). Minimization of non-bonded energy of helical segments of various lengths (up to DP 24) resulted in left-handed helical structures. Glycosidic carbon-proton coupling constants ($^3J_{GH}$) corroborate with the predicted dihedral angles.

Introduction

Although the main structural features of starch and related saccharides are known for many years, research interest in this field - having either academic or industrial character - does not diminish. There are several reasons for that:

1. The problem of fine structure is continuing to be the subject of investigation and speculation. The energy-storing biopolymers amylopectin and glycogen are typical examples. Both polysaccharides are highly branched having high complexity as compared to linear chains. But even in case of amylose, having a predominantly linear structure, conformation in solution, double to single helix formation and chirality have been the subject of numerous recent publications.
2. Improvements in experimental techniques have been remarkable, first of all in instrumental analysis and enzymic methods. In structure determination new results revealed by high intensity X-ray techniques, dynamic light-scattering experiments. Solid state ^{13}C -NMR sufficient resolution for carbohydrate studies and is now used to investigate aqueous aggregation and gelation of amylose. By sophisticated multidimensional pulse techniques high-field NMR measurements in liquid phase give information on solution conformation of various oligo- and polysaccharides.

3. Theoretical calculations and graphical visualization help in structure investigation and evaluation of complex experiments. High-speed work stations are available and semi-empirical methods for energy calculations are now well parametrized for the carbohydrate field.

In this paper we shall concentrate on approaches offered by high-resolution, high-field NMR interpreted by insight derived from theoretical calculations.

Theoretical calculations were introduced already in the 70-es to unveil the energy constraints that govern three-dimensional molecular structures. These were used at first to supplement diffraction analysis. With the advent of fast computers they have become indispensable tools of present-day analytical methods. Computational methods were developed simultaneously to treat even macromolecules including solvent interactions and it is also possible to model their dynamic behavior.

Investigation of starch related polysaccharides in solution, especially in water, is connected with the increased interest in the biological functions of carbohydrates.

NMR techniques were developed relatively lately and were entered into the starch field only recently. The first, and perhaps most important feature revealed by NMR was the increased mobility of oligo- and polysaccharide subunits. Relaxation time determinations were evaluated in terms of the microdynamics and local correlation.

Results and discussion

In connection to all these new developments we report now on our studies on the average conformation of amylose in aqueous solution.

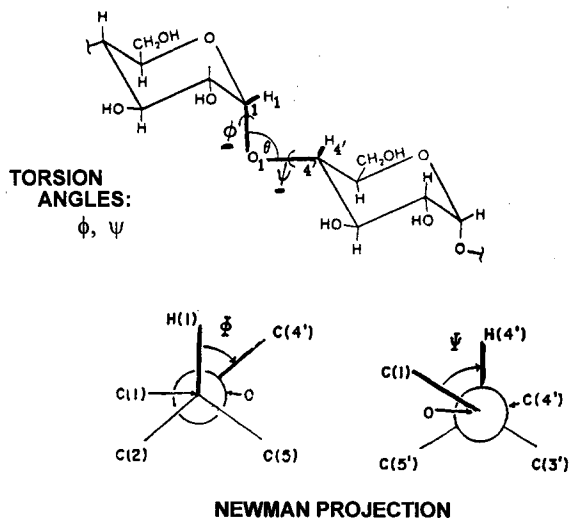


Fig. 1.

High resolution ^1H - and ^{13}C -NMR spectroscopy was chosen as a method because it results in quantities that can be compared to predicted values of theoretical calculations. We concentrated on a conformation dependent NMR parameter: the three-bond glycosidic coupling constants ($^3J_{\text{CH}}$).

Their dependence on the torsion angles is well understood.

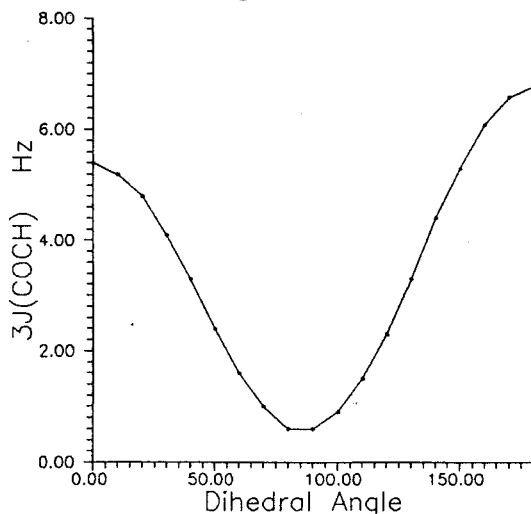


Fig. 2.

Commercial samples of maltooligomers were used for this study and a monodisperse amylose (DP 4800) kindly submitted by prof. Beate Pffannemüller.

Table 1

^1H -NMR chemical shifts [ppm] and vicinal coupling constants [Hz] of amylose (DP 4800) determined at 600 MHz and 80°C in D_2O . Chemical shifts are referred to TMS.

Atom	$\delta(^1\text{H})$	M^a	$^3J_{\text{HH}}$
1	5.350	d	3.9 (J_{12})
2	3.621	dd	9.9 (J_{23})
3	3.938	dd	8.9 (J_{34})
4	3.620	t	9.7 (J_{45})
5	3.819	ddd	2.1 (J_{56a}) 5.1 (J_{56b})
6 _a	3.863	dd	-12.2 (J_{6a6b})
6 _b	3.791	dd	

^a d - doublet, t - triplet, dd - podwójny dublet, itd.

The following results were obtained:

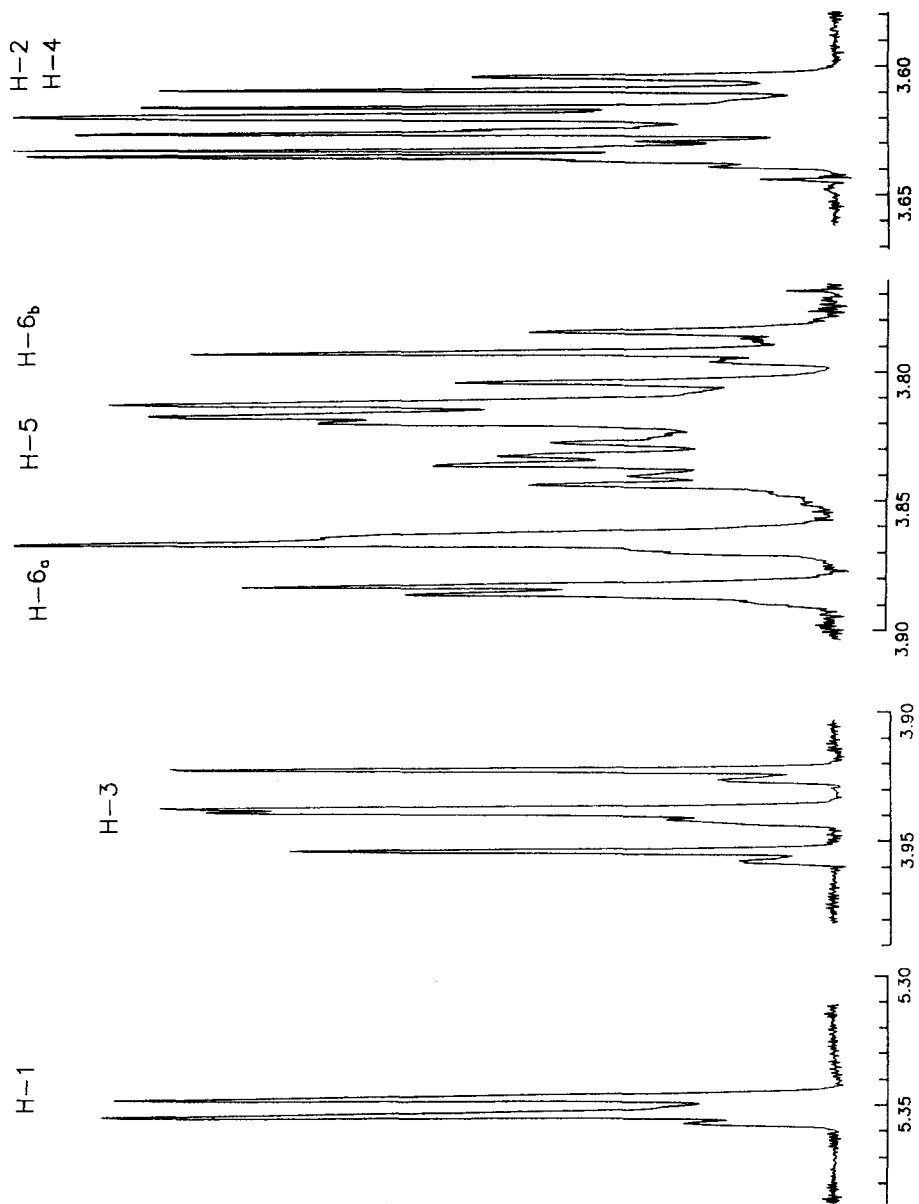


Fig. 3.

Unambiguous assignment of the ^1H -NMR spectrum of the amylose sample was possible only at 600 MHz. Fig. 3 shows all the multiplets of the one-dimensional spectrum. Precise values of proton chemical shifts and coupling constants were derived by analyzing the multiplets by spin-simulation.

These coupling constants are compatible only with the ${}^4\text{C}_1$ conformation of the glucose subunit in each subunit of the oligomer.

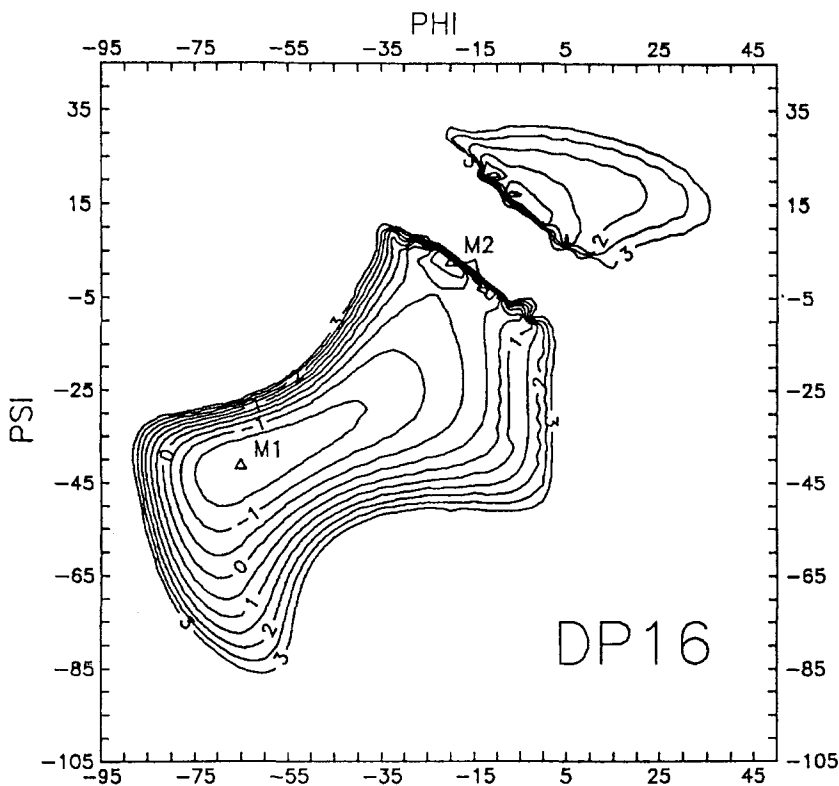


Fig. 4.

Using program CAOS (developed in our Institute) the non-bonded conformational energy of several maltooligomers with various Degree of Polymerization (DP 7, 8, 16, 24) has been calculated in helical conformation as a function of the glycosidic torsion angles (relaxing the hydroxymethyl side chains and without hydrogen bonding or solvent effect). For DP 16 it is represented on Fig. 4 as a relief contour map. M1 and M2 denote the two low-energy minima. Energy maps for different maltooligomers have similar character, only the energy values depend on the DP.

Note that left-handed helices (corresponding to the contour levels at negative Φ and Ψ values) are less energetic than the right-handed ones and are separated from each other by a high potential barrier. The lowest energy right-handed conformation is denoted by M3.

Our experiments verified that:

The NMR parameters are practically independent of the degree of polymerization and they are identical with the chemical shifts of monodisperse amyloses of low (DP 35) and of high molecular weight (DP 4800) - results obtained some years ago in collaboration with dr. Beate Pffannemüller.

Proton-carbon coupling constants of the C-O-C-H type depend on the absolute value of the torsion angle. So they can be used to evaluate the average torsion angles. For ${}^3J_{\text{CH}}$ values found in maltoheptaose (4.6 and 5.3 Hz)

$$4.6 \text{ Hz} \rightarrow \Phi_{\text{H}} (\text{H-1-C-1-O-C-4}') = -26^\circ \text{ (or } 140^\circ) \text{ and}$$

$$5.3 \text{ Hz} \rightarrow \Psi_{\text{H}} (\text{H-4'-C-4'-O-C-1}) = -4^\circ \text{ (or about } 153^\circ)$$

where values in parentheses follow from the double-valued nature of the function (and will be disregarded from energetic considerations). These torsion angles describe a conformation that is not far from the minimum M2.

In case of amylose we found a value of 4.4 Hz for ${}^3J_{\text{C1,H-4}}$. The corresponding Ψ_{H} value (-26°) indicates a similar conformation, not essentially different from that of DP 7 discussed above.

In general in saturated flexible molecules both chemical shifts and vicinal coupling constants are time-averaged values over all possible conformations in solution. Longitudinal relaxation times (T_1) of maltooligomers and amylose prove that local motion of the subunits is very effective for relaxation (despite of the long linear chain) resulting in values of the order 0.2 s (at 75.5 MHz).

Our results determined at 70°C are complementary to those of professor Brant published recently for room temperature and indicate the damping function of the solvent to the local motion.

Conclusions

On the basis of above findings the following conclusions have been drawn:

The average conformation of all glucose subunits in amyloses and various maltooligosaccharides in pure, neutral D20 solution at 80°C can be characterized as the ${}^4\text{C}_1$ conformation.

NMR parameters (chemical shifts, coupling constants) vary only slightly with DP (for the DP values studied). Local motion of the subunits is efficient enough to result T_1 values of about 0.3 s.

Lowest energy minima of single helices having constant pitch but various lengths (between DP 7 and 24) as calculated by the HSEA method were found to have minima in the left-handed region (both the extended and the compact forms).

Glycosidic $^3J_{CH}$ coupling constants and nOe values observed in aqueous solutions are compatible with conformational parameters (Φ_H , Ψ_H) being not far from the compact type minimum (M2). The importance of M2 over M1 is enhanced with increasing DP.

These data support the representation of amylose conformation in solution as a randomly broken helical chain.

KONFORMACJA POLISACHARYDÓW SKROBIOWYCH W ROZTWORZE. BADANIA W WYSOKOPOLOWYM NMR I OBLICZENIA TEORETYCZNE

Streszczenie

Nie maleje zainteresowanie strukturą i konformacją polisacharydów skrobiowych. Ma ono motywacje akademickie i przemysłowe. Roztwory wodne pozwalają na stosowanie nowych technik badawczych.

W pracy podaje się wyniki pomiarów maltooligosacharydów w zakresie magnetycznego rezonansu jądrowego w wysokim polu.

Czasy relaksacji (T_1) atomów węgla (^{13}C) są wysoce elastyczne (0.3 s. w $80^\circ C$).

Minimalizacja energii nie wiążącej dla segmentów heliksu o różnej długości (do DP = 24) sugeruje lewoskrętne struktury. Stałe sprzężenia glikozydowych atomów węgla ($^3J_{CH}$) zgadzają się z przewidzianymi kątami wiązań. ☒

DANUTA M. NAPIERAŁA¹, MARIUSZ POPENDA²

NMR AND COMPUTATIONAL COMPARATIVE STUDY OF THE AMYLOSE – BENGAL ROSE COMPLEXING IN DMSO SOLUTION

Abstract

Proton and carbon NMR spectroscopy was used to study the nature of amylose complexing with Rose Bengal in dimethylsulfoxide. Based on the analysis of chemical shifts changes in NMR spectra under the influence of dye-amylose chain interaction the computer molecular model of the helical amylose - Bengal Rose complex was proposed using the INSIGHT II and MOPAC programmes.

Introduction

Molecular modeling of polysaccharides complexes in solution has been the subject of active research for many years [2-6, 8]. Many biopolymers are poorly water soluble and therefore, they have been studied in such organic solvents as dimethyl sulfoxide (DMSO), carbon tetrachloride, chloroform. Amylose, the linear starch component, with α -(1 \rightarrow 4) - linked D-glucosyl units was one of them. It is well known, that DMSO is an effective amylose solvent and as the strong hydrogen bond acceptor may influence it. Especially, the chain configuration and flexibility are affected, on chemical and physical ways. The chain flexibility induces disordered or random coil states in solution.

It has been suggested that in the neutral aqueous solution amylose behaves as a "random coil" with short, loosely bound helical segments, whereas in DMSO the persistence of intramolecular hydrogen-bonding leads to an increase in the helical content and the compactness of the helical segment [1]. These changes in polymer behaviour due to a solvent affects the reactivity of amylose towards low-molecular compounds and on stability of the complex. Nevertheless there is a question whether dimethylsulfoxide is a good solvent for amylose complex formation because for the most known amylose-iodine complex this solvent suppressed the iodine binding [9].

¹ University of Agriculture, Department of Physics, 60-637 Poznań, Poland

² Institute of Bioorganic Chemistry, Polish Academy of Sciences, 61-704 Poznań, Poland

A complexing effect between amylose and heteronuclear photosensitizer, Bengal Rose in aqueous environment was shown previously [7, 10]. A simple model of the complex formation was proposed [10]. In this report, ^1H - and ^{13}C -NMR spectroscopy data were examined for amylose with Bengal Rose in DMSO-d_6 at different dye concentrations. The molecular model of six-fold amylose helix with associated Rose Bengal molecules in DMSO solution was considered.

Materials and methods

Commercial sample of potato amylose was a product of SIGMA, Bengal Rose (sodium salt) was purchased from ALDRICH Chem. Co. and deuterated solvents, D_2O and DMSO-d_6 , from I.B.J. Świerk/Otwock. Both solutions, of potato amylose and Bengal Rose (BR) in DMSO were blended at high temperature in appropriate proportions to obtain a desired dye concentration, from 5 to 20mM for 1% amylose. The measurements were performed after 24h storing at stable temperature. High resolution ^1H - and ^{13}C -NMR spectra were recorded with a Varian Unity 300 spectrometer operating at 300 MHz. The chemical shifts were measured with external 4,4-dimethyl-4-silapentane sodium sulfonate (DSS) in ^1H -NMR spectra and external dioxane in ^{13}C -NMR spectra. All the computer modeling study were conducted using the INSIGHT II and MOPAC programmes working in the SGI Iris Indigo 2 workstation.

Results and discussion

The effect of a solvent on the amylose - Bengal Rose (BR) complexing in solution was observed in the proton and carbon NMR spectra of both compounds in water and dimethylsulfoxide (Fig. 1). The H-NMR spectra of amylose in DMSO-d_6 exhibited all the resonances of hydroxyl protons [9], the signals for OH-2 and OH-3 strongly deshielded by intramolecular bonding and OH-6, which all disappeared after changing the solvent with D_2O (Fig. 1c). The chemical shift displacement of all the single signals of the amylose proton resonance in the H-NMR spectrum in the presence of Rose Bengal molecules in DMSO-d_6 is presented in Table 1.

At lower BR concentration, only a small paramagnetic effect of 0.02 ppm for OH-6 hydroxyl group signal at $\delta = 4.58$ ppm in the amylose ^1H -NMR spectrum could be observed. This insignificant effect points to lack of any drastic conformational changes in the amylose chain. The dye molecules did not disturb the intramolecular bonding with OH-3 and OH-2 hydroxyl groups in polymer. At low concentration they might cause some restrains for the freedom of hydroxymethylene groups. In the ^1H -NMR spectrum of 1% amylose with a higher Bengal Rose concentration, 10 mM in DMSO-d_6 solution, strong deshielding of OH-2 ($\Delta\delta = 0.08$ ppm) and OH-3 ($\Delta\delta = 0.07$ ppm) signals was observed without change in the OH-6 resonance.

Table 1

Values of chemical shift for amylose proton signals in the ^1H -NMR spectra of 1% amylose with Bengal Rose in DMSO- d_6 solution.

Proton group	Chemical shift δ , ppm		
	without RB	with RB of 5 mM	with RB of 10 mM
OH - 3	5.51	5.52	5.60
OH - 2	5.40	5.41	5.50
H - 1	5.10	5.10	5.11
OH - 6	4.58	4.60	4.61

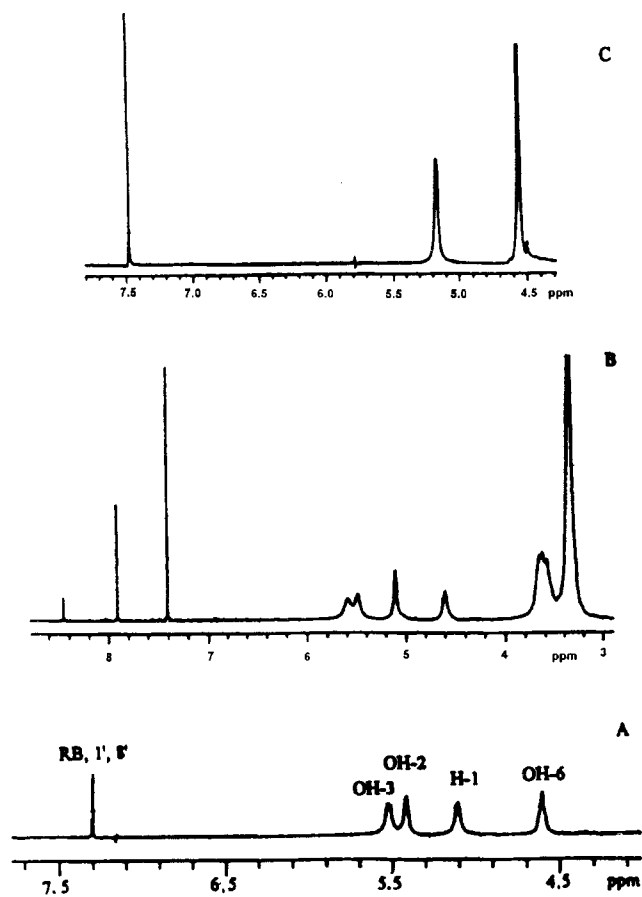


Fig. 1. ^1H -NMR partial spectra of amylose ($c_{\text{AM}} = 1\%$) with Bengal Rose in DMSO- d_6 solution at 298K; BR concentration of 5 mM (A) and 10 mM (B) and in D_2O solution with 20 mM BR concentration (C), at 300MHz.

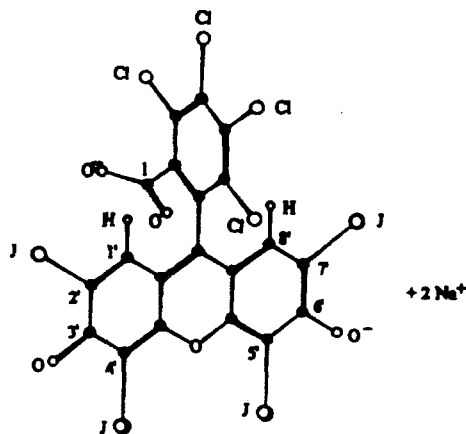


Fig. 2. Molecular structure of 4,5,6,7 - tetrachloro - 2',4',5',7' - tetraiodofluorescein (Bengal Rose).

Bengal Rose (Fig. 2), exhibited the single proton resonance at 7.40 ppm beyond the region ascribed to absorption of the polymer protons in the high resolution ^1H -NMR spectrum (Fig. 1a) at lower concentration range studied. In the dye concentration of 10 mM this signal was resolved into three well separate signals at 8.46 ppm, 7.92 ppm and 7.41 ppm with the intensity ratio equal 0.12 : 0.4 : 1, respectively (Fig. 1b). It suggests a cooperative conformational effect in amylose chain forced by the Bengal Rose interaction, revealing an inhomogeneity of dye molecules state in the system. Taking into account the signal intensity ratio, equal to the ratio of absorbing protons in the proton NMR spectrum, one could obtain the degree of the associated BR molecules per the number of amylose monomer units. Among three NMR Bengal Rose signals observed, the most deshielded signal with the lowest longitudinal relaxation time indicated the most restricted dye molecules. The two other signals with a similar relaxation time might be involved in a cooperative dye interaction in DMSO. From the analysis of the signals the integration ratio suggested that two dye molecules were associated with six monomer units corresponding to the six-fold helical turn. There was no similar dye concentration effect on the ^1H -NMR spectrum of amylose - Bengal Rose in the D_2O solution. A considerable intensity decrease of the signals in the ^1H -NMR spectrum of amylose in the presence of dye and their significant broadening pointed to a reduction of conformational mobility of the polymer due to the complex formation as well as to changes in the proton relaxation time of both compounds.

Nonequivalent dye subsystems were found in the amylose - RB complex in the DMSO-d_6 solution based on the proton NMR spectrum. They also changed the ^{13}C -NMR spectra of both compounds. Effect of the cooperative dye-polymer interaction on

chemical shift displacements of the carbon signals in the system are presented in Fig. 3 and Fig 4. The assignment of the signals of BR and amylose carbon atoms was given in [5, 7]. At high Bengal Rose concentration the signal of the carbonyl group, C(1)OO, at $\delta = 164.3$ ppm split into two signals, both deshielded as compared with the above, of 2.4 ppm and 0.6 ppm, respectively. It confirmed a multiphase dye state in the system. Other bands in the BR carbon NMR spectrum displaced very selectively. A considerable upfield displacement of the signals attributed to the Bengal Rose phenolic ring carbons in the region of 127 - 133 ppm might arise from the penetration of phenolic ring into amylose helix.

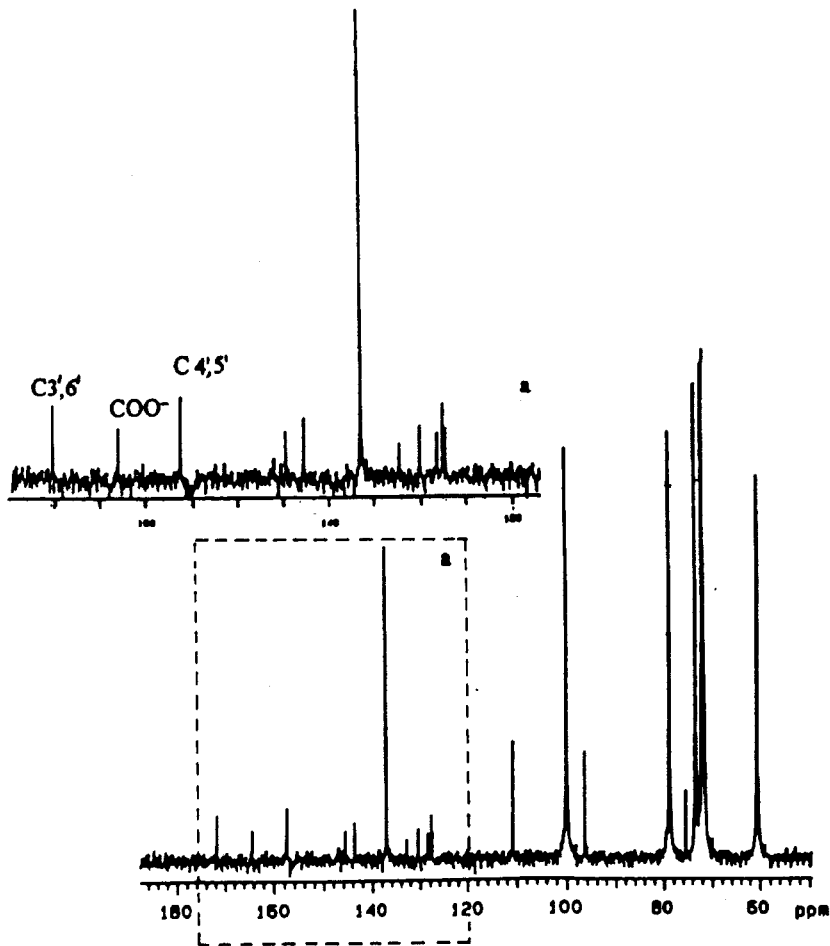


Fig. 3. ^{13}C -NMR spectra of 1% amylose with Bengal Rose of 5 mM DMSO-d_6 solution at 295K.

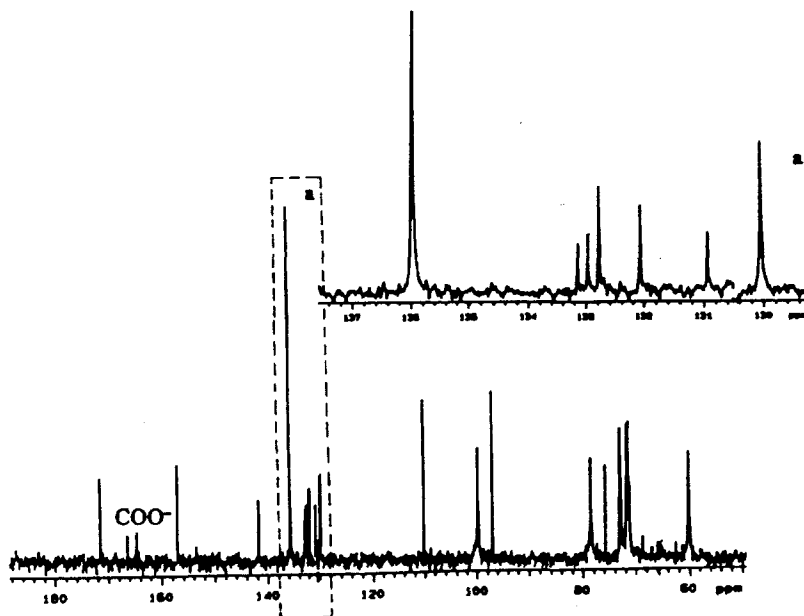


Fig. 4. ^{13}C -NMR spectra of 1% amylose with Rose Bengal of 10 mM DMSO- d_6 solution at 295K.

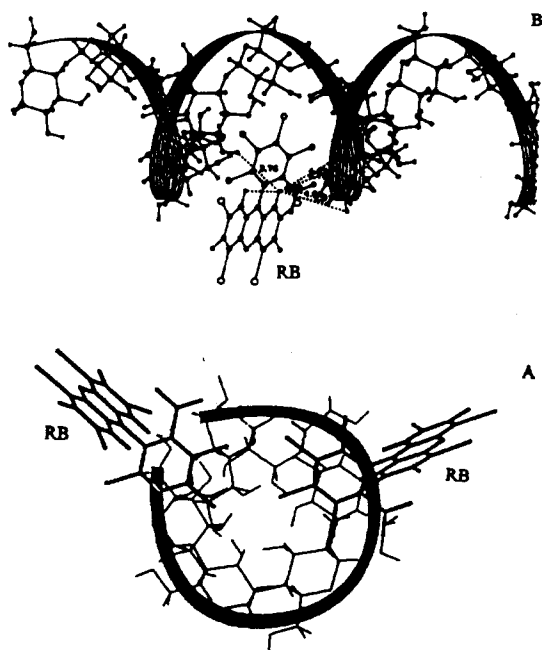


Fig. 5. Molecular model of six-fold amylose chain helix and Bengal Rose complexed in DMSO solution: projection along helical axis with two BR molecules approaching (A) and with one BR molecule (B).

Taking into account results from the ^1H - and ^{13}C -NMR analysis of amylose – Bengal Rose in DMSO-d_6 solution at different dye concentration, a molecular model of amylose helix - dye molecule complex could be proposed in Fig. 5. Bengal Rose molecule approaching the helical chain on the distance of 3 - 4 Å from the nearest polymer atoms, appropriate to hydrogen bonding, was confirmed with the computer simulation program.

Conclusions

The ^1H - and ^{13}C -NMR study of the amylose - Bengal Rose complexing in deuterated dimethylsulfoxide at amylose concentration of 0.01 g/cm^3 and in 5 - 20 mM concentration range of BR showed a cooperative dye - polymer interaction at higher dye concentration. The considerable paramagnetic effect on OH-2 and OH-3 amylose proton signals and carbonyl BR signal splitting in the dublet accompanying the conformational polymer changes proved the role of these groups in conformational constraints. Based on the analysis of the NMR data a computational molecular model of single six-fold amylose helix was proposed with two associated dye molecules through phenolic ring approaching the helical chain.

The work was supported by KBN Grant 5 PO6 G 05408

REFERENCES

- [1] Dais P., *Carbohydr. Res.*, **160**, 1987, 73-93.
- [2] Hardy J., H.Sarko, *J.Comp. Chem.*, **14**, 1993, 848-857.
- [3] Houtman A., M.Atalla, *Plant Physiol.*, **107**, 1995, 977-984.
- [4] Inoue Y., H.Hoshi, M.Sakusai, R.Chujo, *J.Am. Chem.Soc.*, **107**, 1985, 2319-2323.
- [5] Jane J.-L., J.F.Robytt, D.-H.Huang, *Carbohydr.Res.*, **140**, 1985, 21-35.
- [6] Mierke D.F., H.Kessler, *J.Am.Chem.Soc.*, **113**, 1991, 9466-9470.
- [7] Napierala D., M.Popenda, Raport nr 1717/PL, 1996, 242-245.
- [8] Nardin R., M.Vincendon, *Macromol. Chem.*, **189**, 1988, 153-162.
- [9] Peng Q.-J., A.S.Perlin, *Carbohydr. Res.*, **160**, 1987, 57-72.
- [10] Polewski K., W.Maciejewska, *Carbohydr. Res.*, **246**, 1993, 243-251.

**MODELOWANIE KOMPLEKSU AMYLOZA - RÓŻ BENGALSKI W DMSO NA
PODSTAWIE SPEKTROSKOPII NMR**

Streszczenie

Zdolność kompleksowania amylozy z fotoczułym sensybilizatorem różem bengalskim w roztworze DMSO, jak wynika z badań metodami spektroskopii NMR, jest uwarunkowana stężeniem barwnika. Przy stężeniu powyżej 10mM w 1% roztworze amylozy pojawia się efekt przejścia konformacyjnego wymuszonego kooperatywnym oddziaływaniem barwnika. Podjęto próbę komputerowego modelowania kompleksu amyloza - róż bengalski w DMSO przy założeniu pojedynczej helisy i dwóch molekuł barwnika przypadających na sześcioczłonowy zwój. ❖

KRZYSZTOF POLEWSKI

COMPUTER MODELLING OF AMYLOSE HYDRATION PROCESS IN THE PRESENCE OF BENGAL ROSE

Abstract

Simulation program HyperChem (Hypercube Inc., Waterloo, Canada) was used to study the conformational behavior of amylose helices in the presence of water and Bengal Rose. The structure was optimized with a program, which utilizes AMBER molecular force field calculations modified for carbohydrates. Single strand of amylose with the left-handed chirality has lower energy than the right-handed, double helix formed in antiparallel fashion from two left-handed strands. It has the lowest energy compared to other duplex conformation, interhelical stabilization occurs through hydrogen bonding O(2) — O(6) atoms. These results were available from computer calculations *in vacuo* and in the presence of water in the system. In water three hydration sites could be identified at O(3), O(6) and HO(6) for the amylose double helix. Bengal Rose when added to the system was located in the groove of double helix through the interactions of the xanthene structure to hydration sites of amylose, which might be deduced as a disruption of the water structure around the amylose helix.

Introduction

Amylose is a linear polymer formed by α -D-glucopyranose units linked through 1,4-bonds. As a main component of starch it is an important carrier of its physico-chemical properties. The experimental [1, 2] as well as modelled [3, 4] structure of the polysaccharide correlated with their physico-chemical and biological properties. Transition between crystallographical B-type and A-types were observed in dehydration/hydration cycles [5, 6]. Also NMR spectroscopic methods demonstrated the existence of different states of water in amylose. At higher humidities when more than two water molecules per glucose unit were available more mobile, less tightly bound water molecule appeared [7]. Geometry of the amylose double helix was widely discussed in the literature. On the basis of the X-ray fiber diffraction pattern data and computerized molecular modelling Wu and Sarko proposed a right-handed parallel-stranded double helix for both A and B amylose [2, 6]. Schulz et al. [4, 8] investigated

full conformation space of the double helix using potential energy minimization procedure within the framework of molecular mechanics. The results indicated the antiparallel left-handed helix. Experimental evidences exist [1, 3, 9], that environment like water influenced the conformational behavior of amylose. It was the starting point for recalculation of the amylose hydration process in the single and double helix in low dielectric and aqueous environment in the presence of Bengal Rose. The AMBER force field molecular mechanics [10] modified for carbohydrates was used.

Method

The molecular mechanic calculations were performed with the HyperChem (Hypercube Inc., Waterloo, Canada) simulation program. All energy study and the conformational behavior of amylose in water in the presence of Bengal Rose were studied with the Amber force field. The starting structure of amylose, the 16 α -D-glucopyranose oligomer, was built using the Sugar Builder program. The torsional angles Φ and Ψ at the glycosidic linkage were set at 2 and -17 as well as 20 and 5 degrees to get D-oligomer in a helical left or right-handed form.

The Bengal Rose geometry optimization and charges were calculated by the semiempirical PM3 method. During this procedure, the dye was assumed to be in an environment at pH 7. This implies that sodium salt was fully ionized to give Bengal Rose dianion.

Conformational Search option in the HyperChem program was used for the systematic conformational search on the glycosidic linkage. In this procedure Φ and Ψ torsion angles varied in 5° intervals within the whole angular range.

Docking simulation between left and right handed oligosaccharides and with Bengal Rose on the amylose duplex were performed using the Periodic Box option with TIP-3 water molecules. These calculations were conducted with global helical parameters maintained constant.

Results and discussion

Results of the molecular calculation for single and double left and right handed amylose helices, their parallel and antiparallely stranded conformations *in vacuo* and in water are collected in Table 1. It can be noted that a single strand with left-handed chirality had lower energy than that right-handed. As proved by the HYDROGEN BOND Option in the HyperChem program no hydrogen bonding in single helix existed. In case of amylose double helix the lowest energy double helix was formed of two left-handed parallel-stranded conformation and the interhelical stabilization occurred through hydrogen bonding between O(2) and O(6) atoms. When the calculations

are performed in aqueous environment, i.e. in the presence of Periodic Box Option with TIP-3 water molecules the total energy in all cases changed. The calculated energies for right-handed double helices (parallel stranded or antiparallel stranded) had higher energetic minima than their left-handed analogues. Left-handed helices were energetically favorable and differences between them were within 5kJ per unit. It could be noticed that in aqueous solution the hydration pattern could be identified by the single and double helices. The conformation energy in water was minimized under the condition of rigid global helical parameters. This simplification might be justified by much smaller relaxation times for the reorientation of water molecules in comparisons with groups of atoms of the macromolecule. Such behavior regarding hydration of amylose was expected and supported by X-ray diffraction studies [11]. Amylose double helix was supported by periodical formation of intermolecular hydrogen bonds between hydroxyl groups and oxygen atoms and by an arrangement of hydrophobic contacts in the core of the double helix. The hydrogen bonding between appropriate hydroxyl group and oxygen was also evidenced by our calculations. It is also known that an increasing amount of water causes transition from the A-type to B-type conformation of amylose [2, 5]. The hydration pattern displayed by the amylose duplex

Table 1

Total potential energy (kcal) of the amylose and amylose + water systems and in the presence of Bengal Rose (BR). In the double helix data first number is given for parallel and second for anti-parallel strand. A_R and A_L - right-handed and left-handed amylose strand, respectively.

	A_L	A_R	A_L-A_L	A_R-A_R	A_L-A_R
in vacuo	-242	-281	-573 -577	-486 -477	228 266
water	-134	-148	-1019 -994	-921 -893	147 131
water+BR	22	32	-171 -125	-105 -101	725 668

is given in Figure 1. Three identified hydration sites correspond to the polar O3, O6 atoms and the HO6 group. Moreover, a number of water bridges was observed. The O2, HO3, O3 and HO2 moieties were involved in the intrahelical hydrogen bonds and they were less accessible to water molecules. The hydration sites were not energetically equivalent. The O6 group was well exposed to the environment and accounted for the majority of the hydrogen bonds with water. Some competition between O3 and O2 atoms appeared decreasing the hydration in that area of the amylose unit. Thus, all polar groups (except the glycosidic O1 atom) are involved in the hydrogen bonds with water or within the double helix. Thus, a single glucose unit accepted 3 water molecules forming a regular hydration shell around the double helix.

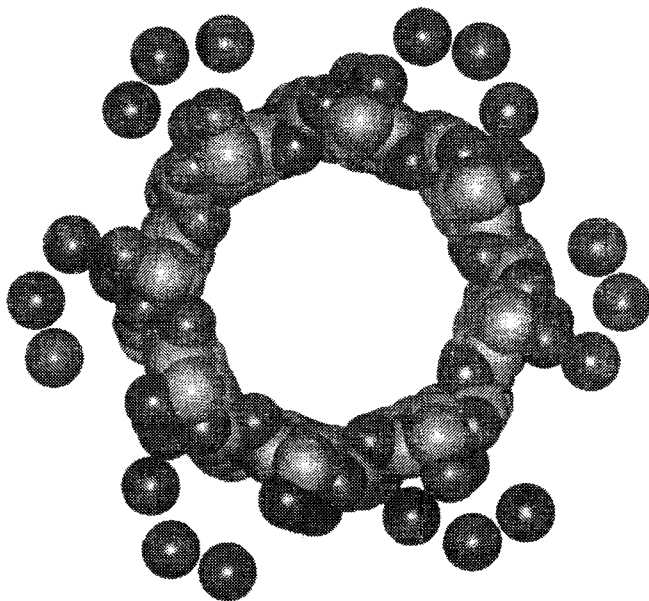


Fig. 1. Segment of the left-handed antiparallel-stranded double helical amylose with the corresponding 3 hydration sites per glucose residue.. The top view of double helix segment of six glucose residues per strand.

When Bengal Rose was added to the amylose double helix system in water the dye located in the groove of double helix through interactions with the xanthene structure as found in docking studies. It was also obvious that the presence of Bengal Rose ruined the water structure around the amylose helix. It is evident from Table 1 the total potential energy of the amylose system in water in the presence of dye was much higher because the presence of the dye disturbed the water-water interactions. Diameter of the amylose helix was large enough to adopt Bengal Rose inside of the amylose helix. However, some hydrophobic interactions inside the helix might preclude such location. It is clear from our previous studies [12, 13] that the presence of Bengal Rose influenced the amylose helix. We suggest that Bengal Rose might interact with amylose either by an intercalation process, adsorption process or the other non-covalent bonding and these calculations seem to confirm our suggestion.

Reported calculation and discussion presented in this paper indicate that the left-handed double helix strand of amylose should be a well soluble species. Because the solubility of amylose can be achieved by boiling at diluted solution we may expect that the complex around 90°C should be either single stranded or in the double helical form

antiparallely stranded and left-handed. In contrast, amylose in nature is insoluble and serves as a glucose storage what indicates that in native state the amylose conformation should be different to provide it to be water insoluble.

Acknowledgement

This work is supported from KBN grant 5 PO6G 054 08

REFERENCES

- [1] Imberty A., Chanzy H., Perez S., Buleon A., Tran V.: *J. Mol. Biol.*, **201**, 1988, 365-378.
- [2] Wu H.-C.H., Sarko A.: *Carbohydr. Res.*, **61**, 1978, 27-40.
- [3] Imberty A., Perez, S.: *Biopolymers*, **27**, 1988, 1205-1221.
- [4] Schulz W., Sklenar H.: *Biopolymers*, **33**, 1993, 1215.
- [5] Dashevsky V. G.: *Conformational Analysis of Macromolecules*; Izdat. Nauka: Moscow, 1987.
- [6] Wu, H.-C.H., Sarko A.: *Carbohydr. Res.*, **61**, 1978, 7-21.
- [7] Lechert H.T.: *Water Activity: Influences on Food Quality*; Academic Press: London, 1981.
- [8] Schulz W., Sklenar H., Hinrichs W., Saenger W.: *Biopolymers*, **33**, 1993, 2145.
- [9] Buleon A., Bizot H., Delage M.M., Multon J.L.: *Starch/Staerke*, **34**, 1982, 361-366.
- [10] Homans S.W.: *Biochemistry*, **29**, 1990, 9110.
- [11] Cleven R., van den Berg C., van der Plas L.: *Starch/Staerke*, **30**, 1978, 223-228.
- [12] Polewski K., Maciejewska W.: *Carbohydr. Res.*, **246**, 1993, 253-265.
- [13] Maciejewska W., Polewski K., Wyspianska-Grunwald M.: *Carbohydr. Res.*, **246**, 1993, 243-251.

MODELOWANIE KOMPUTEROWE PROCESU HYDRATACJI AMYLOZY

Streszczenie

Do zbadania stanów konformacyjnych helisy amylozy w obecności wody i różu bengalskiego zastosowano program do modelowania komputerowego HyperChem (Hypercube Inc., Waterloo Kanada). Badane struktury optymalizowano przy pomocy programu AMBER, wykorzystującego metody mechaniki molekularnej zmodyfikowanej dla węglowodanów. Pojedyncza lewoskrętna spirala amylozy ma niższą energię niż prawoskrętna, podwójna antyrównoległa struktura złożona z dwóch lewoskrętnych spiral posiada najniższą energię w porównaniu z innymi konformacjami dupleksów, a interhelikalna stabilizacja zachodzi poprzez wiązanie wodorowe między atomami O(2) a O(6). Zbliżone wyniki podane powyżej otrzymano zarówno dla obliczeń *in vacuo*, jak i w obecności wody w układzie. W obecności wody znaleziono trzy miejsca na powierzchni helisy, gdzie następuje hydratacja, i są to miejsca przy atomach O(3), O(6) i HO(6). Doadanie barwnika, różu bengalskiego, do amylozy lokuje go w bruzdzie spirali poprzez oddziaływanie struktury ksantenowej z miejscami hydratacji, co może być opisane jako zaburzenie struktury wody wokół helisy amylozy. ☒

KRZYSZTOF POLEWSKI, DANUTA NAPIERAŁA

ABSORPTION AND FLUORESCENCE STUDY OF AMYLOSE COMPLEX IN CATIONIC DETERGENT USING BENGAL ROSE AS A SPECTROSCOPIC PROBE

Abstract

In order to estimate the detergent influence on the process of amylose-dye complex formation the absorption and fluorescence studies of Bengal Rose in the amylose – Bengal Rose complex in the presence of cationic detergent, tetradodecyltriethylammonium bromide, TDABr, were carried out. The fluorescence quenching study allowed to calculate binding constant between the dye and amylose. Thermodynamic parameters were calculated from the temperature dependencies of binding constant. Fluorescence lifetime measurements allowed to determine the environment and distribution of the dye in both systems.

An increasing amount of amylose from 0.1% to 2% led to changes in both, absorption and fluorescence spectra. Observed isosbestic point at 623 nm in the absorption spectrum indicated formation of the static complex between amylose and dye. This was confirmed by the fluorescence spectra where a decrease and shift of fluorescence maximum to longer wavelength was observed. When a cationic detergent above its cmc concentration was added to the system with 1.75% amylose and Bengal Rose the fluorescence maximum shifted to 600 nm and its intensity decreased by 5 times as compared with the system without detergent. Calculated enthalpy and entropy had positive values indicating that not only electrostatic processes took place but also hydrophobic forces participated in the complex formation. Calculated stability constant suggested that the detergent facilitated formation of the amylose complex by the factor of 4.

Introduction

An increasing number of ingredients and additives like food dyes and preservatives [1] as well as environmental impurities modify properties of such significant food component as carbohydrates [2, 3]. The binding complexation of dyes to biopolymers induces changes in the physical properties of dyes. Alterations of the absorption and fluorescence spectra i.e. the fluorescence intensity and emission polarization for many dyes including Bengal Rose were observed [4, 5, 6]. Bengal Rose containing one phenoxide and one carboxylate group, both capable of the reac-

tion with amylose and/or detergent may readily form complexes serving simultaneously as a probe for the dye environment. Amylose and its derivatives can form complexes with a variety of substrates. It has been found that the major factor in such case is due to the substrate hydrophobicity and solvent polarity [7, 8, 9]. The study indicated that hydrogen bonding between host and guest also influenced the stabilization of the helical form of amylose and determined its reactivity with substrates. The interactions also involved complexed molecule located within or on the helical surface of amylose [10]. In this paper, modification of amylose due to properties complexation by detergent and thermodynamic properties of such complexes were studied using spectroscopic methods.

Materials and methods

The following chemicals were used: Potato amylose from POCH Gliwice (Poland) with DP = 120, as measured by light scattering experiment.

Bengal Rose from SIGMA dissolved in water in the concentration of $1 \cdot 10^{-4}$ M as a stock solution. The dye was recrystallized from methanol before used.

Tetradodecyltriethylammonium bromide TDA-Br detergent from SIGMA. The 28 mM stock solution in water was diluted as requested.

Aqueous samples for absorption and emission studies

Amylose solutions (0.1% to 2%) were prepared by digestion of amylose in water at 80°C for 10 minutes then cooled to room temperature. A required amount of detergent and dye was added to them keeping the total volume of the sample of 1 ml. Prepared samples were measured directly after blending then stored at dark at room temperature for further measurements.

Spectral measurements

The absorption spectra of Bengal Rose were measured using HP4 Photodiode Array Spectrophotometer Hewlett-Packard with the 2 nm resolution.

The fluorescence spectra and fluorescence lifetimes of Bengal Rose and UVCD spectra of amylose were taken using UVCD instrument at National Synchrotron Light Source at Brookhaven National Laboratory, at port U9B [11].

Results

Aqueous absorption and emission spectra of Bengal Rose with amylose

Increasing concentration of amylose, from 0.1% to 1% or, from $5 \cdot 10^{-5}$ to $1 \cdot 10^{-3}$ M, in the presence of $2.5 \cdot 10^{-6}$ M Bengal Rose in aqueous solution led to changes in ab-

sorption and emission spectra. The 549 nm band in the absorption spectrum of Bengal Rose decreased and simultaneously shifted to a longer wavelength. For 1% amylose the peak was located at 554 nm as compared with 548 nm in an aqueous solution. The shoulder located at 514 nm was shifted to 520 nm. The apparent isosbestic point at 623 nm corresponded to the complex formation between amylose and Bengal Rose. The ratio of the absorption intensities at λ_{550} and λ_{514} reached 3, pointing to the monomeric form of the dye in that complex.

The aqueous fluorescence spectra of Bengal Rose with increasing concentration of amylose showed a decrease of fluorescence intensity at maximum and a shift of the maximum to a longer wavelength. For 1% amylose the maximum was at 576 nm compared to 570 nm in water. Decreasing fluorescence intensity reflected a static quenching resulting from the formation of the amylose-Bengal Rose complex, whereas the spectral shift suggested that a part of dye molecules was located in the environment of the dielectric constant lower than for water.

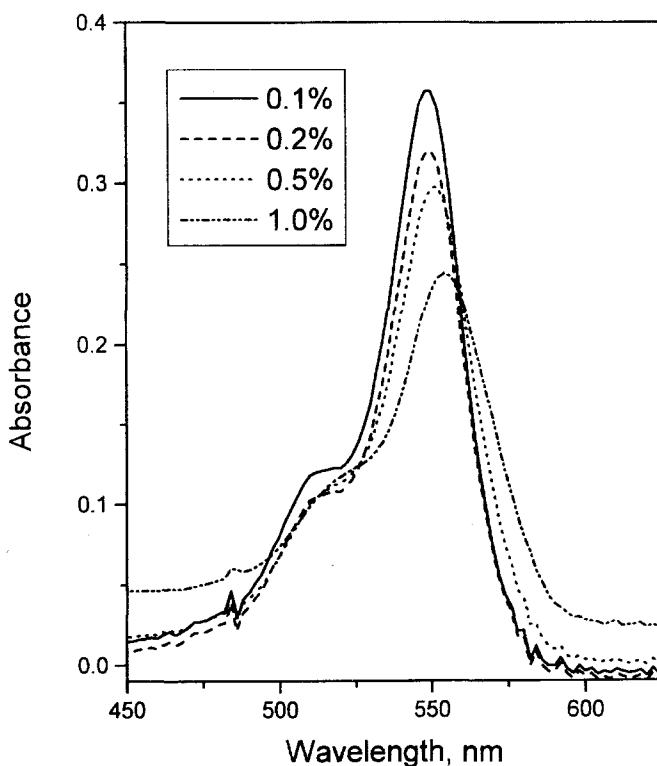


Fig. 1. Absorption spectra of $2.5 \cdot 10^{-6}$ M Bengal Rose in 14 mM detergent, TDABr, versus increasing concentration of amylose. The concentration of amylose is given in the legend.

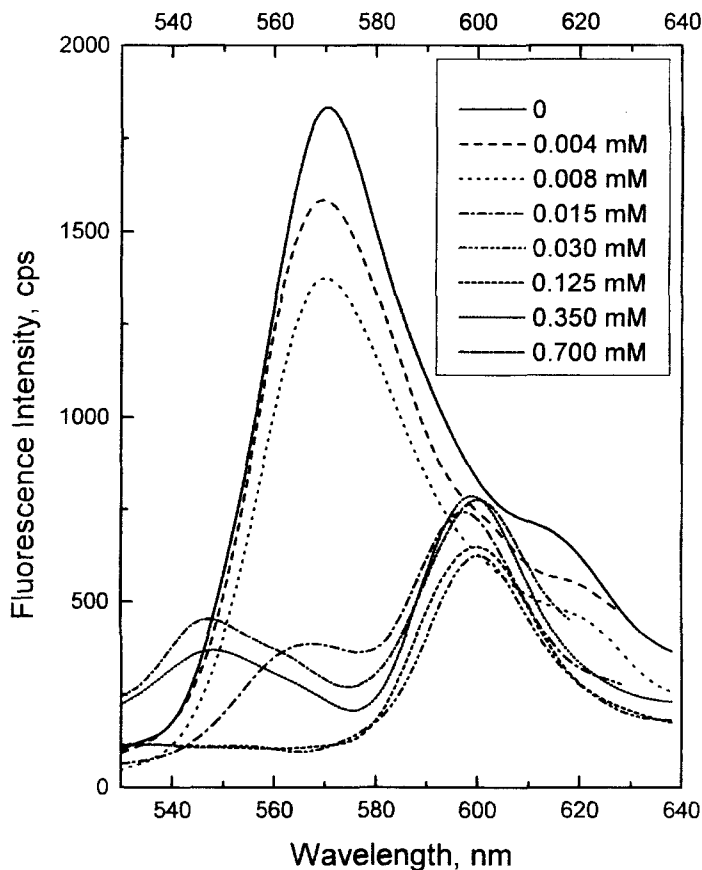


Fig. 2. Fluorescence spectra of $2.5 \cdot 10^{-6}$ M Bengal Rose with 1% amylose at changing detergent, TDABr, concentration, given in the legend, $\lambda_{\text{ex}} = 500$ nm.

Absorption and fluorescence spectra of Bengal Rose with amylose and TDABr

The absorption and fluorescence spectra of Bengal Rose in the system containing 1.75% amylose, $2 \cdot 10^{-6}$ M Bengal Rose and TDA-Br cationic detergent at the concentration changing from 0.7 μM to 0.7 mM are given in Figures 1 and 2. An increasing amount of detergent moved the absorption peak from 548 nm to a longer wavelength and decreased its intensity. These changes were observed only when the concentration of detergent in the system reached 0.1 mM, i.e. when the detergent concentration reached its critical micelle concentration. The fluorescence spectra of Bengal Rose were also altered. Up to 0.1 mM the increasing amount of TDA-Br quenched the fluorescence at 575 nm. Higher detergent concentration dramatically changed the emission

spectrum of Bengal Rose. The maximum emission was shifted to 600 nm and another peak at 550 nm appeared, the fluorescence intensity decreased by five times as compared with the system without detergent. Color of the solution changed from reddish to light-pink. Such behavior might point to at least two physical processes. The first of them could be the static quenching process of the Bengal Rose emission by amylose and detergent and the second, one could deal with the formation of dimers of Bengal Rose molecules which were incorporated into micelles.

Thermodynamic and kinetic results

Disappearance of the color of the solution as well as observed quenching of the Bengal Rose fluorescence during the complex formation provided spectroscopic determination of the stability constant of such complex k_s . At the ratio of BR/Am higher than 1:20, i.e. with an excess of amylose, we might assume that the host to guest ratio in the complex was 1:1 and for absorbance measurements k_s was given by

$$k_s = [A-RB]/[A] \cdot [RB] \quad (1)$$

where: $[A] = [A]_0 - [A-RB]$; $[RB] = [RB]_0 - [A-RB]$; $[A-RB]$ – the concentration of the amylose-Bengal Rose complex.

In case of fluorescence measurements we used Stern-Volmer equation to determine that quenching constant, and k_q was given by

$$F_0/F = 1 - k_q \cdot [Q] \quad (2)$$

where: F_0 and F were intensities of the Bengal Rose fluorescence without and with quencher, respectively; $[Q]$ – was the quencher concentration.

Using the fitting program we could obtain the binding constant for both methods. The calculated values were 2460 M^{-1} and 10100 M^{-1} for amylose with Bengal Rose and, for amylose with the Bengal Rose – detergent system, respectively.

In order to calculate thermodynamic parameters of the above systems the fluorescence measurements were carried out at 10°C , 23°C and 40°C . The calculated values for the free energy, ΔG° , enthalpy, ΔH° , and entropy, ΔS° , are presented in Table 1.

The enthalpy of the process was calculated from the slope of the van't Hoff plot. Both enthalpy and entropy had positive values.

Fluorescence lifetime measurements

In order to determine the location and distribution of the dye in that heterogeneous system the fluorescence lifetime measurements were applied. The fluorescence lifetime of Bengal Rose in different systems is given in Table 2. Bengal Rose in water had only one short lifetime at 90 ps. In 1% amylose solution with the ratio of BR/A up

to 1:222 two components were observed. The first, shorter, with 110 ps indicated that the environment of the dye changed to less polar, and the second, the long one, with lifetime of 3.6 ns but contributing only in 10% to the total decay was characteristic for Bengal Rose in the micellar environment. When the concentration of detergent added exceeded 0.1 mM a 3.6 ns component became the major contribution to the observed decay. Third component appearing at 1.7 ns, indicated a lower dielectric constant of the medium and it was observed as a major component when the detergent in that system was below its cmc.

Table 1

Thermodynamic parameters for the complex formation of amylose with detergent and Bengal Rose as calculated from the fluorescence data.

Temp. °C	Binding const $\text{mol}^{-1} \cdot 10^{-4}$	ΔG° $\text{kJ} \cdot \text{mol}^{-1}$	ΔH° $\text{kJ} \cdot \text{mol}^{-1}$	ΔS° $\text{J} \cdot \text{deg}^{-1} \cdot \text{mol}^{-1}$
10	0.34		48.3	92.3
23	1.1	-22		
40	2.8			

Table 2

Fluorescence lifetimes of Bengal Rose in different systems

	lifetime 1		lifetime 2		lifetime 3	
	ps	α	ns	α	ns	α
BR in water	83	1				
BR + amylose ^a	110	0.95			3.6	0.1
BR + am + det ^b	83	0.49			1.7	0.51
BR + am + det ^c	88	0.03	1.7	0.11	3.7	0.88
BR + det ^b	86	0.96			3.7	0.04
BR + det ^c	85	0.81	0.49	0.19		

^a for amylose concentration from 0.1% to 2%,

^b below cmc of detergent,

^c above cmc of detergent.

Detergent concentration study

As indicated by the data in Table 2 it was obvious that the presence of amylose changed the micellization process of the dye. In order to confirm that amylose influ-

enced the detergent cmc the experiments with and without amylose in the system were carried out. The results are presented in Fig. 3. It is clear from this Figure that the presence of amylose in the detergent solution decreased its cmc by more than one order of magnitude from original 1.4 mM to 8 mM. In that case we might suggest that amylose served as a condensation center for micelization what pointed to more dye molecules located in the micellar environment.

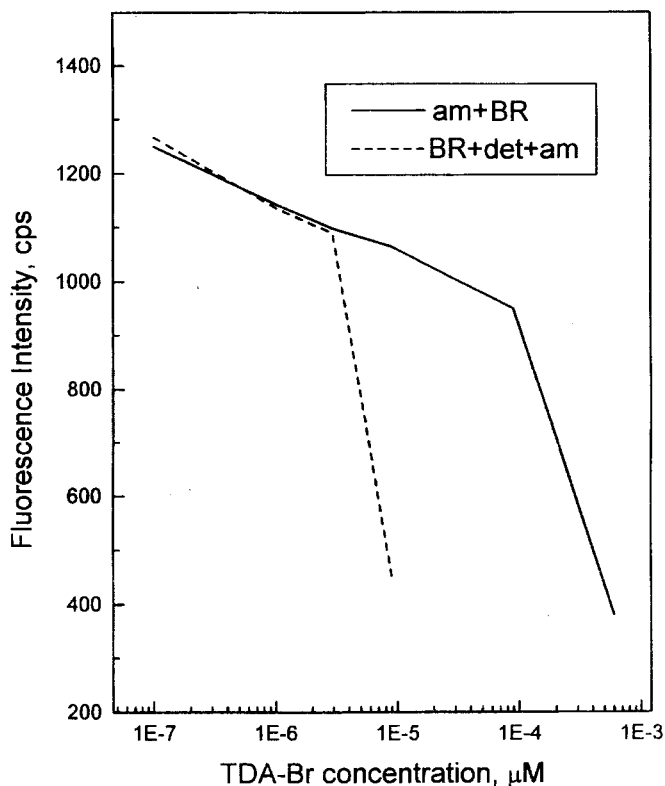


Fig. 3. Fluorescence intensity of $2 \cdot 10^{-6}$ M Bengal Rose without and with 1% amylose versus detergent concentration

Discussion

In the present study the influence of the cationic detergent on the complexation process between amylose and dye was studied. Our previous papers [8, 9, 12] showed that Bengal Rose and amylose chain either formed an inclusion complex or adsorbed on the amylose surface. When cationic detergent was added further changes in the system were observed. Absorbance and fluorescence study showed generally decreasing trend with increasing concentration of amylose and detergent. Additionally, a red

shift relative to aqueous system occurred. All those changes delivered a strong evidence for the complex formation. The stability constant for the amylose-Bengal Rose complex formation, k_q , was 2460 M^{-1} . In the presence of detergent the stability constant was 10100 m^{-1} . It means, that detergent facilitated the complex formation by the factor of 4. The influence of the detergents on the amylose behavior followed a general mechanism where the formation of inclusion complexes involved hydrocarbons [13]. This fact might have serious implications if we assumed that any other detergent-like hydrocarbons which interacted with carbohydrates might increase the ligand uptake like heavy-ion metals or other pollutants.

Whereas a liner Stern-Volmer plot generally indicated an equivalent accessibility of all species of fluorophores present in particular system to the quencher, the exact mode of quenching it is not always clear. In that case contributions from both static and dynamic quenching should be considered. Temperature study was performed to distinguish between two possible quenching. The temperature increase in the range from 10 to 40°C in both cases was paralleled by the S-V quenching constant increase. It suggested a dynamic quenching resulting from increased collisional deactivation. Fluorescence lifetime measurements appeared to be a sensitive tool in resolving the exact contribution of dynamic component. The plot of preexponential factors or the lifetime ratio versus the amylose concentration should give a slope equal to k_q , k_d and k_s quenching constants. Calculated dynamic part was about 20% in both cases and the static part contributed largely to the overall quenching process. Results of this study confirmed the contribution from the static quenching.

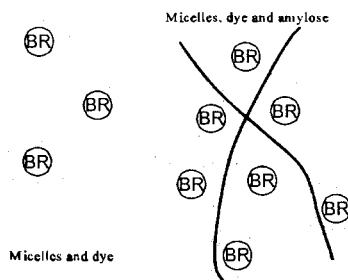


Fig. 4. Schematic representation of the micellization process under absence and presence of amylose.

Detergent concentration study showed that the cationic detergent facilitated formation of the amylose-Bengal Rose complex. Additionally, we might rationalize this process in terms of the detergent induced additional micelisation of the system, i.e. the amylose helix served as a chain around of which the mices were formed. Such bind-

ing in solution might be considered as a consequence of the rigidity loss of the amylose molecules caused by the detergent (see Fig. 4).

These considerations are also supported by thermodynamic parameters given in Table 2. Positive enthalpy value indicated that the hydrogen bonding appeared to be unfavorable and the positive entropy effect indicated the formation of a hydrophobic bond in the system. This might be attributed to the release of the hydrated water molecules from amylose upon binding. Thermodynamic data indicated that the driving force for the dye complexation to amylose in aqueous and micellar solution were electrostatic as well as hydrophobic.

Acknowledgment

This work was supported from KBN grant 5 PO6G 054 08

REFERENCES

- [1] Heijnen M.L., van Amelsvoort J.M., Weststrate J.A.: *Eur. J. Clin. Nutr.*, **49**, 1995, 446-57.
- [2] Wulff G., Kubik S.: *Carbohydr. Res.*, **237**, 1992, 1-10.
- [3] Tezuka Y.: *Biopolymers*, **34**, 1994, 1477-81.
- [4] Neckers D.C.: *J. Photochem. Photobiol., Ser. A*, **47**, 1989, 1-29.
- [5] Rodgers M.A.: *J. Chem. Phys. Letters*, **76**, 1981, 509-514.
- [6] Rodgers M.A.: *J. Phys. Chem.*, **85**, 1981, 3372-3374.
- [7] Hui Y., Gai Y.: *Makromol. Chem.*, **189**, 1988, 1281-1294.
- [8] Polewski K., Maciejewska W.: *Carbohydr. Res.*, **226**, 1991, 179-183.
- [9] Maciejewska W., Polewski K., Wyspiańska-Grunwald M.: *Carbohydr. Res.*, **246**, 1993, 243-251.
- [10] Jiang X.K., Li X.Y., Huang B.Z.: *Proc. Indian Acad. Sci. (Chem. Sci.)*, **98**, 1987, 423-429.
- [11] Polewski K., Kramer S.L., Kolber Z.S., Trunk J.G., Monteleone D.C., Sutherland J.C.: *Rev. Sci. Instrum.*, **65**, 1994, 2562-2567.
- [12] Polewski K., Maciejewska W.: *Carbohydr. Res.*, **246**, 1993, 253-265.
- [13] Bulpin P.V., Cutler N.A., Lips A.: *Macromolecules*, **20**, 1987, 44-49.

POMIARY ABSORPCJI I FLUORESCENCJI KOMPLEKSÓW AMYLOZY W DETERGENCIE KATIONOWYM UŻYWAJĄC RÓŻU BENGALSKIEGO JAKO SONDY FLUORESCENCYJNEJ

Streszczenie

W celu określenia wpływu detergentów na proces powstawania kompleksu amyloza-barwnik przeprowadzono pomiary absorpcji oraz fluorescencji różu bengalskiego w obecności kationowego detergenta bromku tetradodecyltrietyloammoniumowego, TDABr. Pomiary wygaszania fluorescencji różu bengalskiego pozwoliły wyznaczyć stałą tworzenia kompleksu między barwnikiem a amylozą. Parametry termodynamiczne obliczono z temperaturowych zależności stałych tworzenia kompleksu. Pomiary czasów życia fluorescencji pozwoliły na określenie środowiska oraz rozkładu barwnika w badanym układzie.

Ilość amylozy wzrastająca od 0.1% do 2% prowadzi do zmian w widmach absorpcji i fluorescencji barwnika. Pojawienie się przy 623 nm punktu izosbestycznego wskazuje na powstanie kompleksu pomiędzy amylozą a barwnikiem. Ten proces zostaje potwierdzony w pomiarach widm fluorescencji, w których obserwuje się zmniejszenie natężenia oraz przesunięcie maksimum w stronę fal dłuższych. Dodanie kationowego detergenta do układu 1.75% amylozy z barwnikiem powoduje, że maksimum fluorescencji przesuwa się do 600 nm, a natężenie emisji zmniejsza się pięciokrotnie w porównaniu z układem bez detergenta. Obliczone wartości entalpii i entropii mają dodatnie wartości co stanowi wskazówkę, że oprócz procesów elektrostatycznych w tworzeniu kompleksu uczestniczą także oddziaływania hydrofobowe. Obliczone stałe wskazują, że obecność detergentu czterokrotnie ułatwia tworzenie kompleksu z amylozą. ❖

PIOTR TOMASIK, WŁODZIMIERZ ZAWADZKI

STARCH FLUORESCEIN COMPLEXES

Abstract

Starch with its hydroxylic groups can excite fluorescein. This dye, red when solid and fluorescing when hydrated in aqueous solution exhibited a yellow fluorescence when sorbed on starch. Comparison of the properties of starch - KI₃, starch - fluoresceine, and starch - KI₃ - fluoresceine complexes led to the conclusion that fluorescein formed surface complexes and also entered the amylose helix.

Introduction

Solid fluorescein is a red to brown powder. It develops a bright yellow color with a strong green fluorescence on activation by hydration in an aqueous solution [1]. We have assumed that also the hydroxyl groups of starch could activate fluorescein.

Starch is known for its ability to accept selectively various dyes. This selectivity results from the starch granule structure, i. e. starch morphology as well as from the dye nature (see review by Tomasik and Schilling [2] and references therein). According to Kobamoto [3] basic dyes adsorb to a greater extent on larger starch granules whereas acid dyes perform better on small granules. This observation does not apply to potato starch [4, 5]. The sorption of certain dyes on starch allows to distinguish between crystallographic patterns of starch (Acridine Orange) [6], to determine the distribution of positive and negative charges in starch granules (Acridine Orange, Erythrosine) (7), determination of α -amylose in starch (Congo Red) [5, 8] and {2-[2-(4-hydroxy-6-methylpyrimidylazo-4-sulfochlorido)]-1-naphthol} [9]. The sorption of dyes on starch changes some properties of dyes. Thus, the fluorescence of Acridine Orange becomes concentration dependent [10], and Methylene Blue could be protected from fading [11]. The sorption heats of Direct Scarlet B and Chrysophenine G on starch are hardly 29.3 and 62.8 k J/mol, respectively [12]. Nevertheless, the sorption of certain dyes on starch is sufficiently strong for application of such complexes for coloring of artificial threads as shown for several sym-triazine dyes [13].

The mode of sorption of dyes on starch is only partly recognized. It is suggested that the sorption involves not only surface of granules but also capillaries [14]. Fluorescence and optical rotatory dispersion studies carried out with Bengal Rose and amylose strongly suggest that sorption and helical inclusion complexes are formed [15]. The Pal [16, 17] studies on induced dichroism of starch-iodine-Methylene blue and starch-iodine-Acridine Orange complexes have led to the conclusion that starch-iodine helical complex is wrapped inside of an additional helix formed by these dyes.

In this paper the studies on the sorption of fluorescein on potato starch i. e. on a combination of amylose and amylopectin are presented.

Materials and methods

Materials

Potato starch manufactured in Niechlów Potato Enterprise in Poland in 1994. Fluorescein, the product of B.D.H.

Ethanol 99.9% manufactured by Polmos Cracow.

Methods

Starch - fluorescein complexes

They were prepared by an immersion of starch (1 g) in ethanolic solutions (100 cm³) containing subsequently 0.010, 0.050, 0.100, 0.250 and 0.500 g of fluorescein and refluxed for 8 hrs. After cooling to room temperature the reaction mixture was filtered off and filtrate of known volume was analyzed for the noncomplexed fluorescein content. The UVVIS, UV2101PC Shimadzu spectrophotometer was used. The absorbance was measured at 496 nm. The calibration curve was drawn based on the absorbance estimations for 10^{-3} , 10^{-4} , $2 \cdot 10^{-4}$, $5 \cdot 10^{-4}$, 10^{-5} , $2 \cdot 10^{-5}$ and $5 \cdot 10^{-5}$ M ethanolic fluorescein solution.

Starch - iodine complex

It was prepared according to Pal and Pal [17].

Starch-iodine-fluorescein complex

Starch-iodine complex (7 g) was refluxed for 5 hrs in 10^{-4} M ethanolic fluorescein solution (100 cm³). Cold reaction mixture was filtered off and dried in the air.

Fluorescence at elevated temperature

Samples of starch - fluorescein complexes were heated at 150 and 250°C for up to 3 h, and at 300°C for 1 h and their fluorescence was checked with UV lamp at 254 and 366 nm.

Thermal analysis

All samples of plain potato starch and its complexes (200 mg in every case) were thermally analysed in the air in the range of 20 to 400°C with corundum (8 mm) as the standard. The Paulik-Paulik-Erdey 1500 instrument made in Hungary was used.

Results and discussion

The experiments showed that starch formed complexes with fluorescein but the guest molecule (fluorescein) uptake by starch reached around 10% of the amount available for the complexation (see Table 1).

Table 1

Attempted and achieved composition of starch - fluorescein complexes

Amount of fluorescein in 1 g of starch	
Attempted	Achieved
in 10 ⁻³ M	
15.40	3.12
7.67	1.91
3.04	1.09
1.62	0.20

The complexes were bright yellow demonstrating that fluorescein in the complex was in its excited state. Temperature tests were carried out in order to distinguish between water and the hydroxylic groups of starch glucose units capable of the excitation of fluorescein. The bright yellow fluorescence of the complexes started to vanish just on either 3 or 1 hour heating at 250°C and 300°C, respectively. The samples turned gradually brown and brown regions of the complex did not fluoresce.

It is commonly accepted and experimentally proved [18] that starch maintained at 130°C for 2 hours was free of adsorbed water. Thus, the parameters at which the fluorescence of complexes ceased eliminated the participation of water in the excitation of fluorescein.

The excitation of fluorescein in contact with starch strongly suggested that surface sorption complexes were formed. However, such circumstance did not eliminate a possibility of the parallel formation of helical complexes. Polewski and Maciejewska [15] proved the formation of such starch complexes with Bengal Rose being structurally close to fluorescein. Therefore, the formation of the complex of starch blue the helical starch - KI₃I₂ complex [2] with fluorescein was attempted. The contact of starch blue with fluorescein gave a brown solid. The appearance of the product sug-

gested that the fluorescence of fluorescein ceased due to common heavy atom effect on the fluorescence [19]. It is likely that such effect could be observed provided that iodine was pushed by fluorescein out of the helical envelope and formed a brown surface complex with starch [20]. Such possibility was examined based on thermograms (TG, DTG, DTA) of plain starch, starch- fluorescein complexes, starch - KI₅ complex, and starch - KI₅ - fluorescein ternary complex. The complexation of fluorescein with starch did not affect the thermogram of plain starch. The decomposition peaks of fluorescein were hidden under strong peaks of starch. Contrary to it fluorescein strongly affected the thermogram of starch blue (Fig. 1).

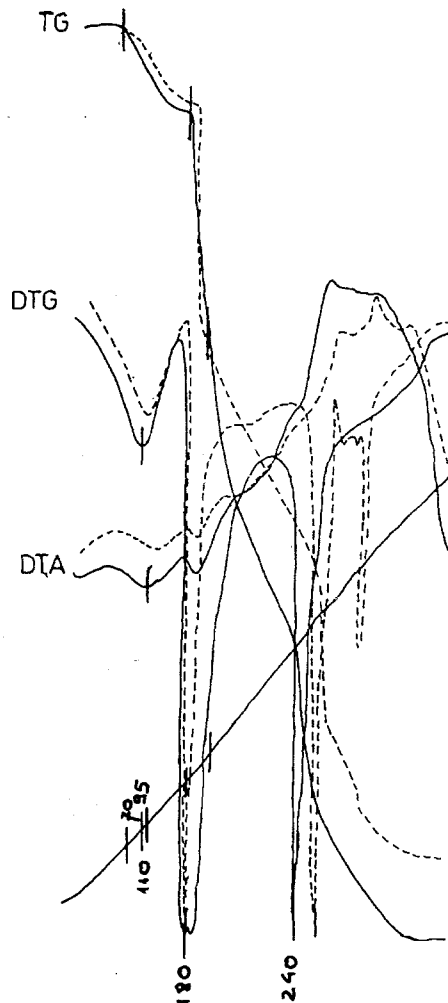


Fig. 1. Thermograms of starch - KI₅ complex, solid lines, and starch - KI₅ - fluorescein complex, broken lines). Thermograms of plain starch and its complexes with fluorescein are identical.

Iodine within the amylose helix decreases the thermal starch stability. Addition of fluorescein increased this stability, although the latter is lower than that of the starch fluorescein complex as shown also in Table 2.

Table 2

Thermal analysis, TG, DTG, DTA, of starch-fluorescein, starch - iodine and starch - iodine - fluorescein complexes, and fluorescein

Complex	Characteristics ^a
Starch - fluorescein ^b	TG: 70 (beginning of the weight loss); 70-145, (-15%); 145-235 (-15.5%); 235-265 (-65%); 265-365 (-87%). DTG: 95s↓; 240vs↓; 355sh,w; 395s↓. DTA: 110b,w; 180vw; 195vw; 215vw; 240w.
Starch- KI ₃	TG: 60 (beginning of the weight loss); 60-155 (-8.5%); 155-165 (-35%); 165-330 (-66%); 330-350 (-78%); 350-400 (-87%). DTG: 95s↓; 155vs↓; 340vs↓; 370w↓; 400s↓. DTA: 110b,w; 160w; 205vw; 245sh; 260sh; 295vw; 370w; 400sh.
Starch - KI ₃ - fluorescein	TG: 60 (beginning of the weight loss); 60-150 (-10%); 150-315 (-69%); 315-460 (-93%). DTG: 95s↓; 165vs↓; 315vs↓. DTA: 110b,w; 165w; 225sh; 270sh; 280sh; 295sh.
Fluorescein	TG: 275 (beginning of the weight loss); 275-360 (-8.5%). DTG: 295w↓; 350vs↓. DTA: 250b,w; 295w; 350sh; 390vw.

^a The data for TG, DTG and DTA are given in °C. The arrow down denotes the endothermic process. The values in parentheses following the TG data show the total weight loss up to the end of the indicated interval. The other symbols introduced are as follows: s - strong; vs - very strong; w - weak; vw - very weak; b - broad; sh - a shoulder.

^b The thermograms are identical for all starch - fluorescein complexes regardless their fluorescein content.

Also the differences in the course of the weight loss (the TG-curve on Fig. 1) suggests that the iodine was liberated from the complex on fluoresceine addition. In the latter case the weight loss is easier and faster.

Conclusion

Starch formed with fluorescein surface and helical complexes. Due to excitation with the starch hydroxylic groups complexed fluorescein fluoresce.

REFERENCES

- [1] Stepanov B.I.: Vvedeniye v khimiyu i tekhnologiyu organicheskikh krasitelei, (Polish transl.), WNT, Warszawa, 1980, p. 198.
- [2] Tomasik P., Schilling C.H.: Adv. Carbohydr. Chem. Biochem., 52 (in the press).
- [3] Kobamoto N.: Rykyu Daigaku Nogakuto Gakujutsu Hokoku, 27, 1980, 139-47; Chem. Abstr., 95, 1981, 78619q.
- [4] Zografi G., Mattocks A.M.N.: J. Pharm. Sci., 52, 1963, 1103-5.
- [5] Schoch T.J., Meinwald E.C.: Anal. Chem., 28, 1956, 382-7.
- [6] Badenhuizen N.P.: Staerke, 17, 1965, 69-74.
- [7] Badenhuizen N.P.: Staerke, 29, 1977, 109-14.
- [8] Katz J.R., Weidinger A.: Z. Physik. Chem., A 168, 1934, 321-3
- [9] Ono M., Sudo Y.: Jpn. Kokai Tokkyo Koho, JP 01,137,998, 1989; Chem. Abstr., 112, 1990, 51758s.
- [10] Czaja A.T.: Staerke, 17, 1965, 69-74.
- [11] Tomita G., Takeyama H.: Kagaku, Tokyo, 28, 1958, 308-10.
- [12] Suda Y., Shirota T.: Sen-i-Gakkaishi, 17, 1961, 414-20; Chem. Abstr., 55, 1961, 17014.
- [13] Courtautts Ltd., British Pat., 977,586, 1964; Chem. Abstr., 62, 1965, 7930.
- [14] Ranbold C.N.: Proc. Am. Assoc. Textile Chem. Colourists, 1935, 247-50; Chem. Abstr., 29, 1935, 6064.
- [15] Polewski K., Maciejewska W.: Acta Aliment. Pol., 17, 1991, 345-50.
- [16] Pal M.K., Roy A.: Macromol. Chem., Rapid Commun., 6, 1985, 749-54.
- [17] Pal M.K., Pal P.K.: Makromol. Chem., 190, 1989, 2929-2938.
- [18] Richter M., Augustat S., Schierbaum F.: Ausgewahlte Methoden der Staerkechemie, Fachbuch Verlag, Leipzig, 1968.
- [19] Jaffe H.H., Orchin M.: Theory and Applications of Ultraviolet and Visible Spectroscopy, J. Wiley, New York, 1954.
- [20] Kudła E., Tomasik P.: Starch/Die Staerke, 44, 1992, 253-260.

KOMPLEKSY SKROBI Z FLUORESCEINĄ

Streszczenie

Skrobia może wzbudzać fluoresceinę swymi grupami hydroksylowymi. Barwnik ten jest czerwony w fazie stałej, ale fluoryzuje po zhydratowaniu i wykazuje żółtą fluorescencję po osadzeniu na skrobi. Porównanie właściwości kompleksów skrobi z KI_5 , skrobi z fluoresceiną i skrobi z fluoresceiną KI_3 prowadzi do wniosku, że fluoresceina tworzy kompleksy sorpcyjne i wchodzi też do wnętrza heliksu amylozy. ☒

MARK F. ZARANYIKA, EDWARD MUKUDU, ALBERT T. CHIRENJE

**ACTIVATION ENERGY FOR THE SALT CATALYZED
HETEROGENEOUS DILUTE ACID HYDROLYSIS
OF THE DIFFICULTLY ACCESSIBLE PORTIONS
OF MICROCRYSTALLINE CELLULOSE**

Abstract

The apparent rate constants, K_c , for the heterogeneous dilute acid hydrolysis of the difficulty accessible portions of microcrystalline cellulose in 0.3 M, 1.0 M and 1.3M HCl containing 0.00 M, 0.08 M and 0.20 M KCl at 60, 70, 75 and 80°C were determined by the loss-in-weight method, and the activation energy, E_a , calculated from the $\ln K_c$ versus $1/T$ curves, where T = absolute temperature. When hydrolysis was carried out in 0.3 M HCl only, a value 25 of kcal obtained for E_a . In the presence of KCl as added electrolyte E_a was found to be constant with a average value of $12.6 = 0.5 \text{ kcal} \cdot \text{mole}^{-1}$, and, in the range of concentrations studied, did not depend on the concentration of the added electrolyte. A possible mechanism to account for the low activation energy is presented.

Introduction

The heterogeneous dilute acid hydrolysis of cellulosic materials is characterized by an initial fast rate of hydrolysis in the "amorphous" region of the material, which then decreases until a constant value is reached in the crystalline portion of the material. The slow rate of hydrolysis in the crystalline portion has been attributed to (a) the intensity of inter- and intra-chain H-bonds, and (b) restrictions to the conformational changes necessary for the hydrolytic reaction to occur [1].

The "amorphous" region of cellulose is often assumed to be "freely" accessible to the hydrolysing medium, so that the Arrhenius activation energy calculated from the temperature dependence of the rate of hydrolysis in this region corresponds to that associated with breaking the glycosidic bond in the cellulose chains. The activation energy for the hydrolysis of the crystalline portion, on the other hand, should include an additional quantity of energy related to the breaking of inter and intra-chain H-

bonds, as well as energy required to overcome restrictions to conformational changes necessary for hydrolysis to occur [1-3].

Different rate laws have been proposed for the heterogenous hydrolysis of cellulose. Meller⁴ proposed a zero order rate law for the hydrolysis of the difficultly accessible portions of cellulose when determined by the loss-in-weight method:

$$\frac{dx}{dt} = k \quad (1)$$

where x = % loss in weight, t = time and k is a constant represented by the slope of the straight portion of the rate plot. Using this law Meller obtained activation energies of 28-29 kcal/mole for the hydrolysis of cotton linters, acetate grade pulp and viscose grade pulp. Nelson³ used the same rate law to show that for cotton linters, mercerized cotton, decrystallised cotton and viscose rayon, the apparent activation energy for both the amorphous and crystalline regions ranges from 31.5 to 33.0 kcal/mole.

When the extent of hydrolysis is followed by the change in degree of polymerization (DP), it was found that data on change in DP with duration of hydrolysis fitted an empirical hyperbolic equation of the type:

$$\frac{1}{kt} = \frac{1}{P_t - P_o} + \frac{1}{P_m - P_o} \quad (2)$$

where k is the empirical rate constant applicable over the entire range of extent of reaction, P_t is the DP at time t , P_o is the initial DP, and P_m is the level-off DP (LODP). Using this empirical rate law Nelson [3] obtained average activation energies for cotton linters and rayon of 30 and 34 kcal/mole respectively. Similar approaches were used by several workers prior to Nelson. Sharples [2] used this approach and obtained activation energies of 31 kcal/mole for the homogeneous hydrolysis of cellobiose and 28 kcal/mole for the accessible fraction in cotton and 38 kcal/mole for the crystalline portion of cotton. Foster and Wardrops obtained a value of 38 kcal/mole for the crystalline fraction of halocellulose. Gibbons [6], and Higgins [7], obtained values ranging from 27 to 35 kcal/mole for different cellulosic materials.

Although there is some variation in the values of E_a reported for different cellulosic materials and different acids used, it is now commonly accepted that the activation energy for the homogeneous acid hydrolysis of cellulose is 28-29 kcal/mole [8]. This is attributed to the energy required to break the glycosidic bond. The activation energy for the hydrolysis of the crystalline region is about 38 kcal/mole, since additional energy is required to break H-bonds in addition to the glycosidic bonds. The energy of an H-bond is often between 3 and 9 kcal/mole [8].

Zaranyika and his co-workers [9, 10] demonstrated that the rate of the heterogeneous dilute acid hydrolysis of cellulose is enhanced considerably by the addition of an electrolyte, and that the kinetics of the reaction can be described in terms of a model based on Donnan's theory of membrane equilibria. According to this model, the rate of hydrolysis of the difficultly accessible portion of cellulose is given by:

$$(dp/dt)_c = k_c [H^+]_c [S] \quad (3)$$

$$= K_c "D [H^+]_s [X^-]_s [S] = k_c [H^+]_s [X^-] \quad (4)$$

Where P denotes products, D is the diffusion coefficient of any added electrolyte MX in the solution phase of the system, $[H^+]$, $[X^-]$ and $[S]$ are the hydrogen ion, and counter ion and reaction site concentrations respectively, the subscript C and S denotes cellulose and solution phases of the system respectively, K_c is a "form factor" relating the diffusion coefficient, D' , of the added electrolyte in the cellulose phase of the system to D, the diffusion coefficient of the electrolyte in the solution phase of the system, and $k_c = K_c "D$, the apparent rate constant for the reaction.

From the brief review above it is apparent that the effect of added electrolyte on activation energy for the hydrolysis of cellulose has not been studied. The aim of the present work was therefore to study the effect of added electrolyte on the activation energy for the hydrolysis of the crystalline regions of microcrystalline cellulose. The effect of changing the concentration of the added electrolyte used are also investigated.

Experimental

Equipment

The equipment used in these experiments was described previously [9].

Materials

The following materials were used: MN - cellulose powder 300 for thin layer chromatography with average particle size of 10 μm (Macherey Nagel and Co., U.K.); potassium chloride and hydrochloric acid - A.R. grade.

Procedure

The loss-in-weight method of Meller for the determination of the hydrolysis rate was used in these experiments. The detailed experimental procedures followed were described previously [9]. Percentage loss-in-weight figures obtained are plotted against time in figures 1. The rate of hydrolysis, V_c , given by the slope of the straight portion

of the hydrolysis curve for the crystalline portion is converted to units of moles of glucose per second (Ms^{-1}). The rate constant, K_c^{D} , is calculated (Table 1) and plotted against $1/T$ in figures 2 and 3.

Table 1

Apparent rate constants, k_c , for the hydrolysis of the difficultly accessible portions of microcrystalline cellulose at various temperatures as a function of acid and added electrolyte concentrations

[HCl]	Temp. ($^{\circ}\text{C}$)	k ($\times 10^{-8} \text{ mol}^{-1} \text{ s}^{-1}$)		
		0.00 M. KCl	0.08 M. KCl	0.20 M. KCl
0.3 M.	60	1.02	21.1	17.6
	70	1.53	34.6	29.0
	75	3.82	56.9	36.6
	80	9.90	63.2	52.6
1.0 M.	60		2.7	1.4
	70		4.6	8.7
	75		6.2	12.2
	80		7.9	12.6
1.3 M.	60	0.86		
	70	1.10		
	75	2.20		
	80	2.30		

Results and discussion

Figures 1 to 3 show that the plot of $\ln k_c$ versus $1/T$ for the crystalline portion of cellulose is linear. We conclude therefore that the hydrolysis of the difficultly accessible portion follows an Arrhenius type equation. E_a values calculated from the slope of the $\ln k_c$ versus $1/T$ curves are shown in table 2. Table 2 shows that when hydrolysis is carried out in 0.3M HCl a value of 25 kcal/mole is obtained for E_a , in close agreement with the values of 27-29 Kcals by Meller⁴ reported. When hydrolysis is carried out in the presence of added electrolyte a constant value of E_a of 12.6 kcal/mole is obtained. This appears to be constant irrespective of the concentration of added salt.

Muhlethaler [11] has proposed that crystalline cellulose is composed of cellulose microfibrils, each consisting of 36 cellulose molecule chains from 1 000 to 15000 glucose units. These molecules are oriented in the same direction, are parallel to one another, and are connected by means of interchain or intermolecular H-bonds between OH-3 in one chain to OH-6 in another to form a layer structure in the A-C plane. In addition intrachain or intramolecular H-bonds exist between the hydroxyls on C-2 and C-6, and OH-3 and the pyranose ring oxygen of successive glucose units. In the A-B

plane, the space between the layers, which are held together by weak Van der Waals forces, is hydrophobic, the "amorphous" regions occurring at chain-ends or interruptions in the microfibrils.

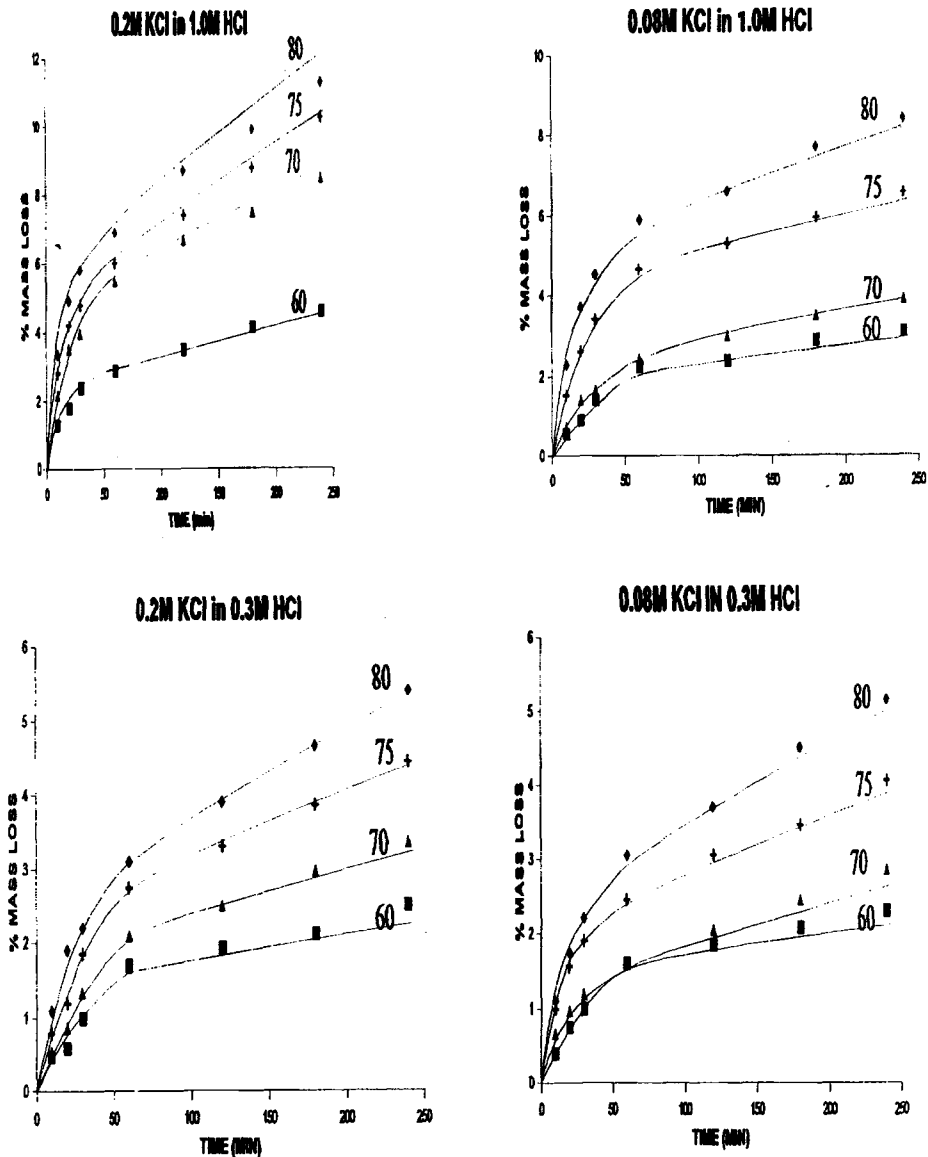


Fig. 1. Plot of percentage-loss-in-weight versus time for the dilute acid hydrolysis of microcrystalline cellulose at different temperatures.

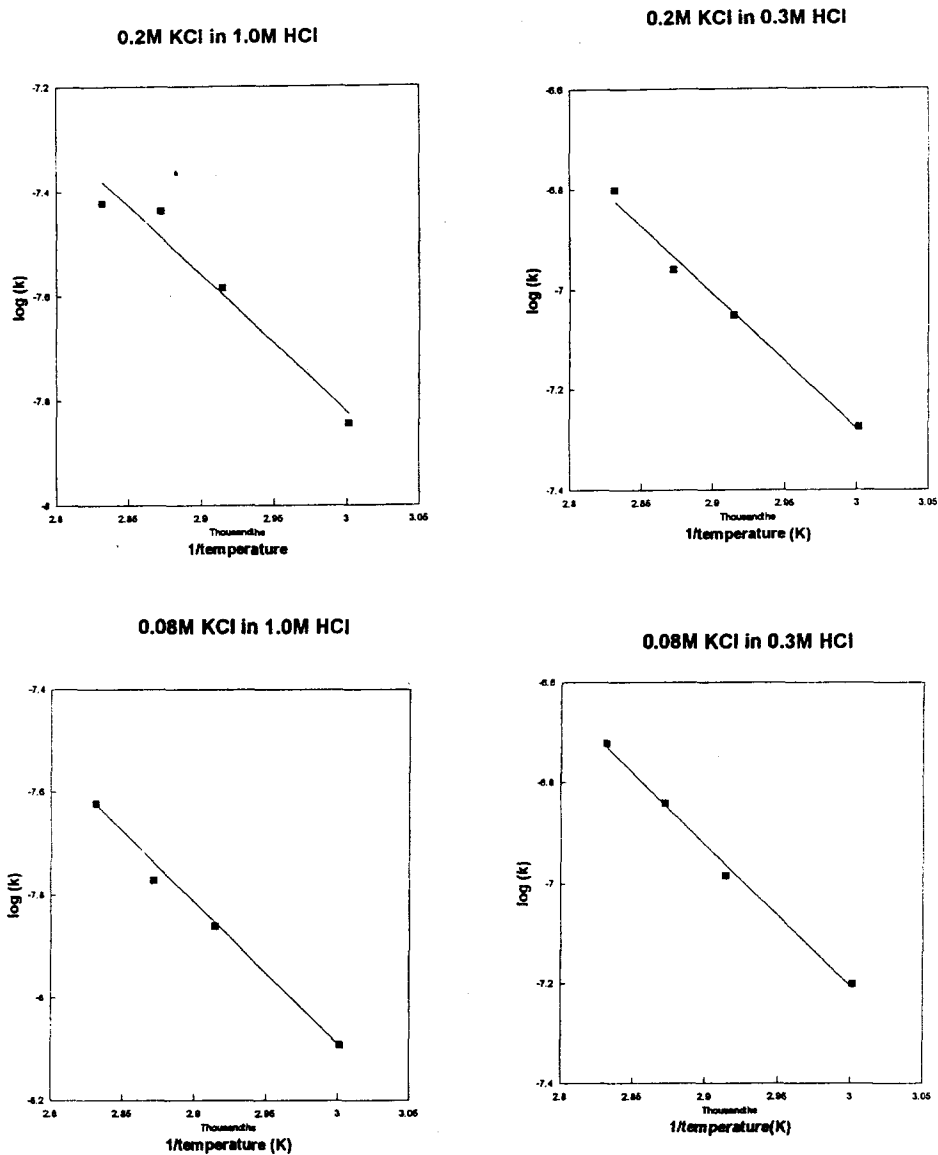


Fig. 2. Plot of $\ln K_c$ versus $1/T$ for the later (straight) portion of the hydrolysis curve (from Fig. 1).

The total activation energy of 25-30 kcal/mole obtained in the absence of the salt catalyst includes the excess energy required to break H-bonds between cellulose chains. The breaking of intermolecular (or inter-chain) H-bonds occurs by intercalation of H_2O molecules into the H-bonds between cellulose chains resulting in inter-crystalline swelling. A notable feature of this inter-crystalline swelling is that from the

crystalline region outwards, the sorbed water molecules become progressively more loosely bound to the cellulose chains, and that even in these regions of more loosely bound water molecules, the intramolecular H-bonds can remain intact depending on the reaction conditions [12].

Table 2

Activation energy values at different levels of HCl and added KCl concentrations

[KCl]	Activation Energy (kcal/mole)		
	1.3 M. HCl	1.0 M. HCl	0.3 M. HCl
0.00 M.		30.7*	25.8
0.08 M.		12.66	13.57
0.20 M.	12.6	12.03	12.43

* Literature value for cellobiose [4].

The activation energy results obtained above throw some light on the mechanism of the hydrolysis of the glycosidic bond in the heterogeneous dilute acid hydrolysis of cellulose. The kinetic model on which the results are based assumes the following elementary steps [9]:



where S is the reaction site and P denotes products. Since heterogeneous dilute acid hydrolysis of cellulose involves breaking intermolecular H-bonds, intra-molecular H-bonds and the glycosidic bonds, S can be (a) the intermolecular H-bond, (b) the intra-molecular H-bond, or (c) the glycosidic bond, as shown in table 3, where the corresponding reactions are indicated.

As discussed in the preceding paragraph the activation energy study results obtained in the present work can distinguish between (a) and (c), but cannot distinguish between (a) and (b), or (b) and (c). Nevertheless, assuming the minimum activation energy of 12-13 Kcal relates to the breaking of the glycosidic bond, then since this activation energy is close in magnitude to the activation for breaking H-bonds, we conclude that the activated complex involved is the protonated glycosidic bond, and that the formation of products, P, from this complex must involve even lower activation energy step(s).

Two mechanisms were proposed for the hydrolysis of glycosides by Edward [13] and Bunton et al. [14] respectively. The mechanism proposed by Edward involves protonation of the oxygen of the aglycone and the formation of a cyclic carbonium-oxonium ion as the rate determining step. Bunton et al proposed a mechanism initiated

by protonation of the ring oxygen followed by formation of an acyclic carbonium ion intermediate again as the rate determining step. Both mechanisms are not consistent with the low activation energy of 12-13 kcal/mole obtained in the present work. The formation of the carbonum-oxonium ions is expected to involve high activation energy in order to break the C-O bond, and to overcome restrictions to conformational changes necessary for the formation of these ions [3, 4].

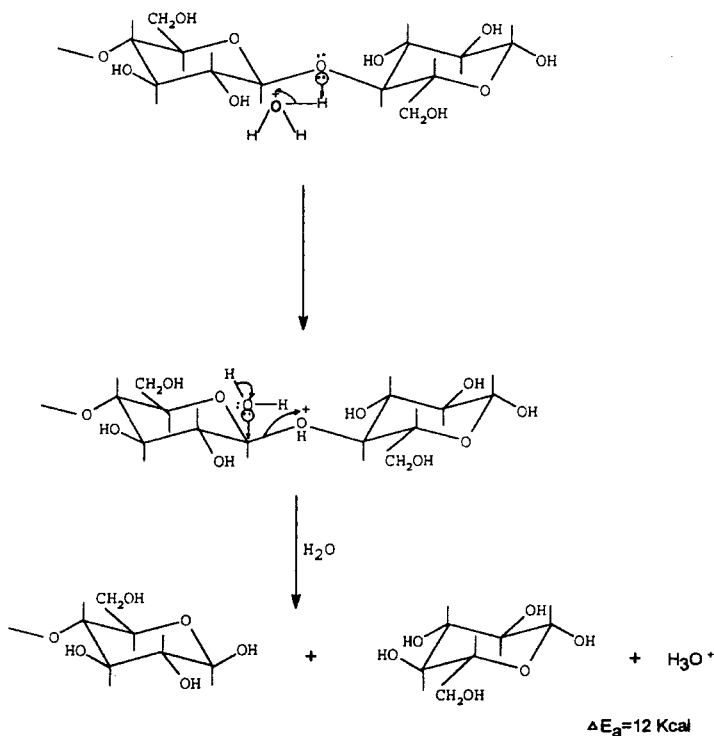


Fig. 3.

Table 3

Types of reaction sites in heterogeneous dilute acid hydrolysis of cellulose

S	Reaction
a. Inter-molecular H-bond	Intercalation of H ₂ O
b. Inter-molecular H-bond	Intercalation of H ₂ O
c. Glycosidic bond	Hydrolysis

The mechanism in Figure 3 would be consistent with the low activation energy of 12-13 kcal/mole obtained in the present work, and is put forward as a plausible mechanism for the hydrolysis of the glycosidic bond in cellulose. In heterogeneous dilute acid hydrolysis of cellulose, the glycosidic bond can be approached by the hydroxonium ion in the A - C plane only because the space between cellulose layers in the A - B plane is hydrophobic. This means that the glycosidic bond is protected by the intra-molecular H-bonds between the hydroxyls on C-2 and C-6, and OH-3 and the pyranose ring oxygen. In turn the intramolecular H-bonds are protected by the inter-molecular H-bonds. For breaking intermolecular H-bonds penetration of the H_3O^+ ions into the crystallites is very slow and, in the absence of added salt, is rate limiting. Addition of an inert electrolyte catalyses the penetration of the H_3O^+ ions into the crystallites and the breaking of the glycosidic bond becomes rate limiting. Further support of the mechanism proposed above comes from the fact that high levels and rates of hydrolysis are obtained when heterogeneous dilute acid hydrolysis of cellulose is carried out under pressure [15].

Table 1 shows that the rate constant for the salt catalysed heterogeneous dilute acid hydrolysis of cellulose decreases as the concentration of the added electrolyte increases. The rate constant, $k_c = k_c^0 d$ (see eqn 4), is identifiable with the flux of the hydrolysing medium into the crystallites. By definition the flux is given by

$$\text{Flux} = \text{Mobility} \times \text{concentration} \times \text{total driving force}$$

The total driving force is composed of an electrical term and an osmotic term. The electrical term is the basis of the Donnan Theory, and has a positive effect on the rate constant, i.e. an increase in the electrical term should lead to an increase in the rate constant. The osmotic term on the other hand tends to reduce the flux of the hydrolysing medium into the crystallites, so that at high electrolyte concentrations, the rate constant begins to drop as the effect of the osmotic term becomes greater than the effect of the electrical term. In previous paper we showed that this point is reached at a concentration of 0.028 molar added salt in the case of Li Cl catalyst [10].

Acknowledgements

This work was supported by a grant from the Research Board of the University of Zimbabwe.

REFERENCES

- [1] J.N. Bemiller: *Adv. Carbohydr. Chem*, **22**, 1967, 25-108.
- [2] A. Sharples: *Trans. Faraday Soc.*, **53**, 1957, 1003-1013; **54**, 1958, 913-917.
- [3] M.L. Nelson: *J. Polym. Sci.*, **XLIII**, 1960, 351-371.
- [4] A. Meller: *J. Polym. Sci.*, **IV**, 1949, 19-28.

- [5] D.H. Foster, A.B. Wardrop: Australian J. Sci. Res., **A4**, 1951, 412-422.
- [6] G.C. Gibbons: J. Textile Inst., **43**, 1952, T25-T37.
- [7] H.G. Higgins, V. Goldsmith, A.W. Mc Kenzie: J. Polymer Sci., **32**, 1958, 57-74.
- [8] H.G. Higgins, V. Goldsmith, A.W. Mc Kenzie: J. Polymer Sci., **32**, 1958, 247-252.
- [9] M.F. Zaranyika, M. Madimu: J. Polym. Sci.: Polym. Chem. Ed., **27**, 1989, 1873-1882.
- [10] M.F. Zaranyika, P. Moses, T. Mavunganidze: J. Polymer Sci., Polym. Chem. Ed., **28**, 1990, 3565-3574.
- [11] Muhlethaler, Pulp and Paper Chemistry and Technology, 1, 3rd Rd, J.P. Casey, ed, Wiley Interscience, N.Y. 1980, p. 13.
- [12] R.D. Kremer, D. Tabb: Intern. Lab., **19**, 1989, 40.
- [13] J.T. Edward: Chem. Ind. (London), 1955, 112.
- [14] C.A. Bunton, T.A. Lewis, D.A. Llewellyn, C.A. Vernon: J. Chem. Soc, 1955, 4419.
- [15] A.J. Beardsmore, Comm. Eur. Communities (Report) EUR 9347, 1984, 432-436.

**ENERGIA AKTYWACJI KATALIZOWANEJ SOLAMI HETEROGENNEJ HYDROLIZY
ROZCIEŃCZONYM KWASEM TRUDNO DOSTĘPNYCH CZĘŚCI
MIKROKRystalicznej CELULOZY**

Streszczenie

Wyznaczano pozorne stałe szybkości, K_c , heterogennej hydrolizy rozcieńczonym kwasem trudno dostępnych części mikrokrystalicznej celulozy w 0,3, 1,0 i 1,3 M kwasie solnym zawierającym 0,00, 0,08 i 0,20 M KCl w 60, 70, 75 i 80°C posługując się metodą ubytku wagi. Energie aktywacji E_a obliczono z krzywych $\ln K_c - 1/T$ gdzie T jest temperaturą absolutną. Gdy hydrolizę przeprowadzano w 0,3 M kwasie solnym otrzymano dla E_a zaledwie 25 kcal/mol. Wobec dodanego KCl jako elektrolitu E_a nie zmieniała się, a średnia wartość $12,6 = 0,5$ kcal/mol i w badanym zakresie była niezależna od stężenia dodanego elektrolitu. Przedstawiono prawdopodobny mechanizm odpowiadający za niską energię aktywacji. ☒

DANUTA SUCHARZEWSKA¹, JULIA KOMINIĄK²,
KRYSTYNA NOWAKOWSKA¹

MODIFIED STARCH-BASED PREPARATIONS WITH ANTISEPTIC ACTION

Positive clinical effects in treatment wounds with iodofors depend to a large extent on physicochemical properties of iodine complexes. They include a high ability to swelling and absorbing liquids. Therefore, studies on improvement of iodofors concern the applicability for iodine complexing of such carriers which under the influence of liquids do not dissolve but swell and, at the same time, release active iodine.

The aim of the study was to obtain a Polish starch-based iodine preparation which could be used in treating surface wounds on skin.

In the investigations potato and corn starch was used. Two types of starch were characterized by different ratios of amylose to amylopectin (1:4, 4:1, respectively). Starch modification consisted of etherification, cross-linking of the etherified starch, and complexing with iodine. During the starch etherification, conditions for production of carboxymethyl starch were determined. This starch was characterized by low viscosity (below 50 Pas), and water retention coefficient (RE) reaching about 5.

The best results were obtained for corn starch with increased amylose content, when the etherification was carried out using monochloroacetic acid in a hydrated medium. In order to obtain the preparation in the form of gel, the carboxymethyl starch was cross-linked. The cross-linking was performed using epichlorohydrin. The best gel quantity and quality were obtained when the cross-linking of corn carboxymethyl starch was performed in a dispersion for 20 hrs at 50°C. Attempts to form an iodine complex of the cross-linked carboxymethyl starch were made using 1.5% solution of iodine at variable time of iodination (1 to 5 hours). It was found that the best iodisorbs were obtained from the corn starch containing over 40% of amylose. ☒

¹ Institute of Chemical Technology of Food, Technical University of Łódź

² Polfa Kutno Farmaceutical Company

Informacja dla Autorów

Pragniemy przekazać Państwu podstawowe informacje, które powinny ułatwić pracę redakcji i ujednolicić wymagania wobec nadsyłanych materiałów.

1. Będziemy na naszych łamach zamieszczać zarówno oryginalne prace naukowe, jak i artykuły przeglądowe, które będą miały ścisły związek z problematyką żywności.
2. Planujemy również zamieszczać recenzje podręczników i monografii naukowych, omówienia z naukowych czasopism zagranicznych, sprawozdania z konferencji naukowych itp.
3. Prace prosimy nadsyłać w 2 egz. (format A4, maksymalnie 30 wierszy na stronie, 60 znaków w wierszu) w maszynopisie; przy pracach napisanych na komputerze prosimy dołączyć dyskietkę z plikiem oryginalnym oraz z plikiem w formacie TXT.
4. Objętość prac oryginalnych, łącznie z tabelami, rysunkami i wykazem piśmiennictwa nie powinna przekraczać 12 stron.
5. Na pierwszej stronie nadesłanej pracy (1/3 od góry pierwszej strony należy zostawić wolną, co jest potrzebne na uwagi wydawniczo-techniczne) należy podać: pełne imię i nazwisko Autora(ów), tytuł pracy, nazwę i adres instytucji zatrudniającej Autora(ów), tytuł naukowy.
6. Publikacja winna stanowić zwięzłą, dobrze zdefiniowaną pracę badawczą, a wyniki należy przedstawić w sposób możliwie syntetyczny (dotyczy oryginalnych prac naukowych).
7. Do pracy należy dołączyć streszczenia w języku polskim i w języku angielskim. Streszczenia powinny zawierać: imię i nazwisko Autora(ów), tytuł pracy i treść – maksymalnie 10 wierszy.
8. Nadsyłane oryginalne prace naukowe powinny zawierać następujące rozdziały: Wstęp, Materiał i metody, Wyniki i dyskusja, Wnioski (Podsumowanie), Literatura.
9. Literatura powinna być cytowana ze źródeł oryginalnych. Spis literatury winien być ułożony w porządku alfabetycznym nazwisk autorów. Każda pozycja powinna zawierać kolejno: liczbę porządkową, nazwisko i pierwszą literę imienia autora(ów), tytuł pracy, tytuł czasopisma, rok, tom, strona początkowa. Pozycje książkowe powinny zawierać: nazwisko i pierwszą literę imienia autora(ów), tytuł, wydawnictwo, miejsce i rok wydania, tom. Informacje zamieszczone w alfabecie niełacińskim należy podawać w transliteracji polskiej.
10. Tabele i rysunki winny być umieszczone na oddzielnych stronach. Rysunki powinny być wykonane na kalce tuszem lub wydrukowane na drukarce laserowej. Każdy rysunek powinien być numerowany kolejno na odwrocie ołówkiem, należy również podawać nazwisko Autora i tytuł pracy, w celu łatwiejszej identyfikacji. Podpisy rysunków należy podać na oddzielnej stronie.
Rysunki wykonane za pomocą komputera prosimy dołączyć na dyskietce w formacie TIF lub WMF.
11. Materiałem ilustracyjnym mogą być również fotografie, wyłącznie czarno-białe.
12. Korektę prac wykonuje na ogół redakcja na podstawie maszynopisu pracy zakwalifikowanej do druku, uwzględniając uwagi recenzenta i wymagania redakcji. W przypadku daleko idących zmian, prace będą przesyłane Autorom.
13. Za prace ogłoszone w naszym kwartalniku Autorzy nie otrzymują honorarium, natomiast otrzymują egzemplarz autorski.
14. Materiały przesłane do redakcji nie będą zwracane Autorom.

ISSN 1425-6959

Warunki prenumeraty

Szanowni Państwo,
uprzejmie informujemy, że przyjmujemy zamówienia na prenumeratę naszego kwartalnika, zarówno Czytelników indywidualnych, jak i od instytucji, co powinno Państwu zapewnić bieżące otrzymywanie kolejnych wydawanych przez nas numerów. Pomimo zmieniających się kosztów druku, jak i objętości naszego kwartalnika Prenumeratorom zapewniamy stałą cenę 5 zł (nowych) za jeden egzemplarz w tym roku. Natomiast cena poszczególnych numerów będzie ustalana według aktualnych kosztów.

Zamówienia na prenumeratę, jak i na poszczególne numery prosimy kierować na adres Redakcji:

PTTŻ Oddział Małopolski

Redakcja Kwartalnika

„ŻYWNOŚĆ. TECHNOLOGIA. JAKOŚĆ.”

31-425 Kraków, Al. 29 Listopada 46

Nr konta: PKO BP I O/Kraków 35510-164353-132